Active layer microbial inocula restore missing functions across thawed permafrost soils

Sylvain Monteux[1,2,3,4], Ellen Dorrepaal[5], Sébastien Fontaine[6], Konstantin Gavazov[7], Sara Hallin[8], Jaanis Juhanson[8], Frida Keuper[9], Josefine Walz[5], Rica Wegner[2], Birgit Wild[2,3], Eveline J. Krab[1]

1: Department of Soil and Environment, Swedish University for Agricultural Sciences, Uppsala, Sweden
2: Department of Environmental Science, Stockholm University, Stockholm, Sweden
3: Bolin Centre for Climate Research, Stockholm University, Stockholm, Sweden
4: Tromsø Museum, UiT The Arctic University of Norway, Tromsø, Norway
5: Climate Impacts Research Centre, Umeå University, Abisko, Sweden
6: Grassland Ecosystem Research Unit, French National Institute for Food, Agriculture and Environment INRAE, Clermont-Ferrand, France
7: Swiss Federal Institute for Forest, Snow and Landscape Research WSL, Birmensdorf, Switzerland
8: Department of Forest Mycology and Plant Pathology, Swedish University for Agricultural Sciences, Uppsala, Sweden
9: BioEcoAgro Joint Cross-Border Research Unit, French National Institute for Food, Agriculture and Environment INRAE, Laon, France

Abstract

Microbial dynamics in thawing permafrost induce a climate feedback of uncertain magnitude. Estimates rely largely on incubations of experimentally-thawed permafrost soils, which may have limited microbial functionality after millennia of frost. In nature, however, seasonally-thawed active layer microorganisms may enter the underlying permafrost soil and introduce missing functions. Here we test the prevalence of functional limitations and how introducing active layer microorganisms can mitigate these across four widespread permafrost soil types. We measure the production of CO_2, CH_4, N_2O, nitrate and ammonium content, bacterial community composition and genes controlling nitrogen cycling. By restoring functions with a diverse microbial community from a temperate grassland, we demonstrate widespread functional limitations in permafrost soils, as CO_2 and N_2O emissions increased across permafrost types over 389 days. However, realistic active layer inocula increased CO_2 or N_2O production less than observed with the diverse microbial community, and not systematically, due to unsuccessful coalescence or limitations in the inoculating soil communities themselves. Under anoxia, active layer inocula quintupled CH_4 while decreasing CO_2 production, resulting in a 35% increase in CO_2-eq over six months. Understanding the factors that will lift the functional limitations of permafrost microbial communities will be key to predicting their substantial, yet unaccounted, consequences on the biogeochemistry of the permafrost region.

Introduction

Arctic permafrost soils store large amounts of carbon (C) that can fuel greenhouse gas (GHG) emissions when these soils thaw due to climate change[1,2]. Understanding the feedback between global warming and GHG emissions from these soils is important for climate change mitigation strategies[2–4]. Research efforts have been dedicated to sampling both the perennially frozen permafrost and the seasonally-thawing active layer of soil profiles across the Arctic, to relate soil physical and chemical composition to long-term GHG production through *in vitro* incubation studies[1,2,5,6]. Incubations provide valuable data and insights into remote sites not easily captured by ecosystem-level measurements, which has allowed to model estimates of the permafrost carbon-climate feedback[2,7,8]. However, most incubation studies neglect the role of biotic interactions, notably microbial community assembly and its effects on soil functioning, which appear increasingly important in determining post-thaw permafrost functioning in nature[9–12]. Upon permafrost thaw, microbial community composition often changes substantially[12–14]. This can occur through endogenous changes in the microbial community present in the permafrost under the new environmental conditions[15,16], but also through invasion of surface microorganisms in the newly-thawed permafrost[13,17]. Due to dispersal limitations in permafrost when still frozen[18], local stochastic extinctions are not counteracted by the dispersal of new microbial species from the active layer. Over tens of millennia, this is thought to decrease diversity and functional redundancy of the microbial community, eventually resulting in communities deprived of certain functions, and therefore hampering or losing specific biogeochemical processes[10]. Thus, the nature and rate of biogeochemical processes resulting in net production of the GHGs carbon dioxide (CO_2), methane (CH_4) and nitrous oxide (N_2O) are not only constrained by soil abiotic and climatic factors, but also rely on microbial community composition[19,20], in ways that remain poorly understood in permafrost soils[10,21].

Permafrost occurs across a large part of the arctic and boreal zone [22] and includes different soil types and different durations of frozen conditions. Yedoma deposits occur in regions that were not glaciated during the late Pleistocene (c. 84 – 11.7 ka BP[23]) and are among the oldest permafrost deposits. They store 297 Pg-C and 37 Pg-N (29% of all C and 38% of all N in permafrost[22,24]) and their high ice content puts them at risk of abrupt thaw. Functional limitation of the microbial community was demonstrated in Yedoma permafrost by adding a functionally rich microbial community from a grassland, which introduced new microbial functions that increased CO_2 emissions and introduced nitrification[10]. The production of CH_4 [9] and N_2O [11] also seem affected by such limitations in Yedoma permafrost, and slow growth of specialised microorganisms in very old Yedoma permafrost could explain these findings[25]. In contrast to the restricted geographical extent of Yedoma, most present-day permafrost, such as those found in palsa peat bogs and sedge-derived peat, or in cryoturbated

soils where frost-induced soil movements actively bury organic matter, were formed after the Last Glacial Maximum and have thus experienced perennial frost for a much shorter time. Cryoturbated soils are widespread and store up to 46% of permafrost C [1,26], and peat permafrost soils store 18% and 7% of permafrost C and N despite their limited and decreasing extent[22,26,27]. How much of these C and N stocks will be converted to greenhouse gases after thaw is of great interest considering the consequences for climate feedbacks (e.g. refs. [21,28–30]), but it remains unclear whether functional limitations have also developed in more recent permafrost, or if functional limitations are common for production of different GHG across permafrost types.

Upon natural thaw of permafrost soils, the introduction of microbial functions would need to originate from the microbial communities in the overlying active layer, through e.g., seepage of ground water during gradual deepening of the active layer, or mixing of soils due to thermokarst. This local active layer community can be functionally diverse, but it may also lack certain functions[31], or may not successfully establish into newly-thawed permafrost. Ice-rich deposits such as Yedoma are found below various types of overlying vegetation, and their high ice content renders them susceptible to abrupt thaw leading to soil layers mixing, which could expose them to a variety of active layer microbial communities. Although post-thaw microbial community dynamics are now actively studied (e.g. refs. [17,21,32]), it remains unclear whether different active layer microbial communities can introduce potentially missing or lost functions to different thawing permafrost types and thereby alleviate functional limitations. If biogeochemical processes in permafrost are governed by microbial functional limitations, this implies that changes in processes would largely depend on changes in microbial community composition.

We compared the occurrence of functional limitations of CO_2, N_2O and CH_4 production across four common permafrost types of different origin and ages (palsa peat, tussock peat, cryoturbated soil and Yedoma sediment), and tested the ability of active layer microbial communities to alleviate such limitations, through two incubation experiments. In the first experiment, we incubated permafrost soils from a palsa peat bog, a sedge peat from moist acidic tussock tundra, and a cryoturbated soil, under oxic conditions for 389 days and compared dynamics of CO_2 and N_2O production and nitrogen (N) pools when incubated with a soil microbial inoculum from their own active layer, a functionally rich microbial community from a temperate grassland as in ref. [10] (positive control), and no microbial inoculum (negative control). Yedoma sediment was incubated alongside the other soils with negative and positive controls as well as all three active layer inoculum types to compare their potential within this type of deposit. In the second experiment, we incubated palsa permafrost under anoxic conditions for 175 days to explore whether inoculation with its own active layer microbial community would stimulate anaerobic GHG production. We hypothesize that 1) microbial communities limit

biogeochemical processes in all permafrost types – although older permafrost deposits may be more strongly affected –, 2) active layer microbial communities can restore or stimulate processes by introducing missing functions, and 3) microbial community coalescence ('invasion' or 'establishment') events should be observed wherever functional limitations are detected.

Methods

Soil collection

The four studied permafrost soils (Figure 1A) comprise a cryoturbated soil, a tussock tundra sedge peat, a *Sphagnum* palsa peat (both histels) and a Yedoma sediment that together represent the main pools of permafrost soil organic carbon (SOC). Samples from these permafrost soils types and their corresponding active layers were taken in 2012 or 2015 using a SIPRE corer (Jon's Machine, Fairbanks, Alaska, USA) or a concrete drill bit (⌀ 10cm) mounted on a gasoline-powered engine. Physical and chemical characteristics of the permafrost and active layer soils are given in Supplementary Table S1. The Cryoturbated soil was sampled from the rim of a non-sorted circle (frost boil) in the Alaskan North Slope (Franklin Bluffs, 69.6685N, 148.7329W, 2012, 70-100 cm depth). The sedge peat histel ('Tussock') was sampled from an *Eriophorum vaginatum*-dominated tussock tundra (moist acidic tundra) of the Alaskan North Slope (Ice Cut, 69.0467N, 148.8343W, 2015, 70-100 cm depth). The second histel ('Palsa') was sampled from a *Sphagnum*-dominated ombrotrophic peat bog underlain by silty permafrost (palsa mire) in sub-arctic Sweden (Storflaket, 68.3462N, 18.9714E, 2015, 110-150 cm depth). The Yedoma sediment originated from the Cold Region Research Engineering Laboratory (CRREL) Permafrost Tunnel (Fox, Alaska, USA, 64.9513N, 147.6206W, 2012, 15 m depth). The soil was sampled from the upper silt unit originating from an upper Pleistocene silty deposit, previously described in ref. [10]. Active layer soils (5-15 cm depth) were collected from the same cores as the Cryoturbated, Tussock and Palsa permafrost soils and used later for inoculum preparation. The functionally-diverse soil microbial community used as a positive control ('Positive control') was collected from the surface layer (0-15 cm depth) of a drained Cambisol developed on granitic bedrock at the LTER research site of the French National Research Institute for Agriculture, Food and the Environment (INRAE) in central France (45°43' N, 03°01' E). The site is an experimental grassland, specifically an abandonment-treatment which had not undergone any cutting or fertilization for 15 years prior to soil sampling in the winter 2018-2019. The physicochemical and microbiological properties of this soil have been described before [10,33–35]. All samples were stored frozen (-18 °C) until the experiment.

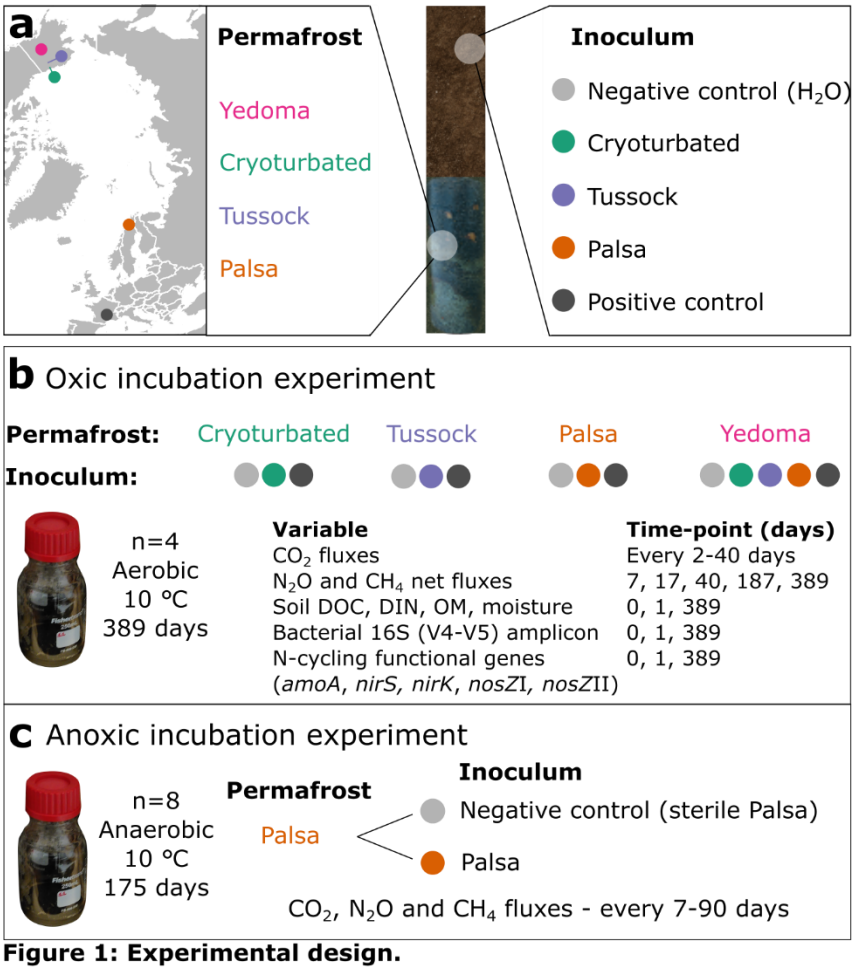

Figure 1: Experimental design.
a) Sampling sites for permafrost and active layer soils.
b) In the oxic incubation experiment, four permafrost soils were inoculated with a positive control from a temperate soil and three with their respective active layer to explore, respectively, whether they harboured functional limitations and whether their active layer microbial communities would alleviate those. All three active layer inoculums were used in Yedoma permafrost, to compare their ability to alleviate functional limitations in Pleistocene-old, deep, ice-rich permafrost.
c) In the anoxic incubation we explored functional limitations of CO_2, N_2O and CH_4 production in the Palsa permafrost.

Experimental design overview

We tested for the existence of functional limitations of CO_2 and N_2O production in four permafrost soils, the ability of active layer microbial communities to alleviate these functional limitations, and whether this can be linked to the communities establishing in permafrost (*oxic incubation experiment*, Figure 1B). This simulates a transfer of soil microbes from the active layer to thawing permafrost by disruptive thaw events (such as active layer detachments or retrogressive thaw slumps), precipitation seepage, or bioturbation, in which newly-thawed permafrost becomes exposed to surface soil microbiomes. Each soil was subjected to three separate inoculum treatments: inoculation (1) with their respective overlying active layer (Cryoturbated, Palsa, Sedge); or (2) with a functionally-diverse microbial community previously used to evidence functional limitations (positive control); or (3) with autoclaved ultrapure water (negative control). As Yedoma permafrost may be exposed to a variety of active layer types upon abrupt thaw, we instead subjected it to inoculation with each of the three

147 active layer soils from the other permafrost types (1), as well as to positive and negative controls (2)
148 and (3). We further tested for the ability of the Palsa active layer microbial community to alleviate
149 putative functional limitations of CH_4, CO_2 and N_2O production in thawing permafrost under anoxic
150 conditions (*anoxic incubation experiment*, Figure 1C). Here, the permafrost was inoculated with its
151 own active layer, and compared to a negative control inoculated with a sterilized sample of its own
152 active layer.

153 Each treatment was replicated four times, resulting in 56 individual flasks ([3 permafrost types × 3
154 inoculation treatments + Yedoma × 5 inoculation treatments] × 4 replicates) per destructive sampling
155 date. Two sets of flasks were prepared to allow a destructive sampling one day after inoculation – to
156 assess putative biases due to inoculation – and at the end of the 389 days of incubation. Flasks were
157 incubated under oxic conditions at 10 °C in the dark. This temperature is in range with the mean
158 active-layer temperatures in Arctic regions during summer and is low enough to be within the thermal
159 tolerance range of psychrophilic microorganisms[36].

160 Net soil CO_2 and N_2O production was quantified on the second set of flasks by measuring cumulative
161 CO_2 production throughout the incubation period and N_2O production rates at several time points (7,
162 17, 40, 187, 389 days). The functional limitation of permafrost microbial communities was defined
163 as a statistically significant ($\alpha = 0.05$) increased in GHG production or a change in N pools in
164 inoculated treatments compared to the negative control. We measured bacterial community
165 composition, abundance, N-cycling functional genes and pH, dissolved carbon and N pools of active
166 layer and permafrost soils immediately after their thawing in the lab, one day after inoculation, and
167 at the end of the incubation to monitor changes in community and functional dynamics.

168 In the anoxic incubation experiment, we incubated the 'Palsa' permafrost soil described above under
169 anoxic conditions and monitored the net change of CO_2, CH_4 and N_2O in the headspace. Each of the
170 negative control and the inoculated treatment was replicated 8 times with one destructive sampling
171 date, resulting in 16 flasks. We incubated all flasks at 10 °C in the dark under a N_2 atmosphere for
172 175 days. We assessed functional limitations of net CO_2, N_2O and CH_4 production by comparing their
173 production rates and cumulative release in the inoculated soil to that of the sterile inoculum control
174 throughout the incubation period.

175 ## Oxic experiment

176 **Permafrost and inocula preparation**

177 The permafrost soils were thawed overnight in a UV-treated and bleached positive pressure hood,
178 then homogenized through an autoclaved 2 mm sieve into a stainless-steel bowl, and excess water
179 was decanted. Approximately 20 g (fresh weight) homogenized soil was set in UV-treated 120 ml
180 incubation flasks, sealed with parafilm to allow for gas but not moisture or microorganism exchange,

and pre-incubated at 10 °C for 11 days before inoculation. Samples of homogenized soil were taken to determine initial gravimetric water content, soil organic matter content (SOM), dissolved organic C (DOC), total dissolved N (TN) and pH (n = 4, except for Tussock moisture and SOM where n = 3 due to low material amount).

We prepared microbial inoculum solutions by submerging active layer soils in autoclaved ultrapure water under a laminar flow hood. Soil slurries were prepared in autoclaved Erlenmeyer flasks with 50 g fresh weight active layer soil. The organic and mineral active layer soils differed in water holding capacity (SI Table S1), therefore we used either 100 ml ('Cryoturbated' and 'Positive control' soils) or 150 ml (organic 'Tussock' and 'Palsa' soils) water. Slurries soaked for 1 hour at 4 °C were shaken for 90 min (150 rpm, orbital), stored overnight at 4 °C, then filtered through qualitative filter paper (Ahlstrom-Munksjö, Eskilstuna, Sweden; 10 µm pore size, previously washed with autoclaved ultrapure water to prevent cellulose leaching). Three samples of each active layer soil were used to determine soil moisture, SOM and pH. One ml of the respective soil suspensions was added to randomly-assigned flasks for each of the four inoculum treatments (Cryoturbated, Tussock, Palsa and Positive control) and one ml autoclaved ultrapure water was added to control flasks. Putative artefacts due to the introduction of labile substrates such as microbial necromass were assessed in a separate incubation and found negligible (Supplementary Material).

Greenhouse gases measurements

To measure CO_2 production rates, headspace air was sampled with a syringe to measure CO_2 concentrations with an infra-red gas analyser (EGM-5 IRGA, PP Systems, USA) throughout the whole incubation period at intervals ranging from 2 to 37 days, keeping $[CO_2]_{v:v}$ below 28,000 ppm to prevent CO_2 poisoning. After measuring, the flasks were flushed with CO_2-free air moisturized with a dew point generator (LI-COR Biosciences, Lincoln, Nebraska) and filtered through a 0.45 µm syringe filter, for >90 s at 1 l min^{-1}, i.e. with at least 10 times the volume of the headspace. CO_2 production rates (τ) were calculated as follows:

$$\tau_i = \frac{[CO_2]_i \cdot \frac{P_i \cdot V}{R \cdot T}}{\Delta t_i}$$

Where τ_i is the rate of CO_2 production per time, $[CO_2]_i$ is the CO_2 concentration at measurement time i, Δt_i is the time interval between measurement ($_i$) and previous flushing, P_i is atmospheric pressure at measurement time i, V the headspace volume of the incubated flasks, R the ideal gas constant and T_i the incubation temperature. Cumulative CO_2 production over the entire 389 days period was obtained by summing up the quantity of CO_2 produced in each flask across all measurements.

Production rates of CH_4 and N_2O were measured at four time points during the incubation: after 15 days, 45 days, 6 months and 389 days. On these days, 13 ml gas samples were taken with a syringe from the headspace – after sampling for CO_2 but before flushing the headspace – and transferred to previously vacuumed 12 ml exetainer tubes (Labco, United Kingdom). The samples were shipped to INRAE facilities in Clermont-Ferrand and analysed for CH_4 and N_2O using a gas chromatograph (GC, Clarus 480) equipped with a photoionization detector (PID, Vici 07709-S). N_2O concentrations between 200 ppb v:v and our lowest technical reference gas of 400 ppb are not included in statistical analyses and only shown for reference, referred to as 'trace amounts'. CH_4 remained below detection limit throughout the oxic incubation experiment.

Soil physical and chemical parameters

Soil chemistry variables - pH, water-extractable DOC, ammonium, nitrate and TN - were measured on the homogenized permafrost soil prior to incubation, one day after inoculation and at the end of the 389 days incubation. About 3 to 5 g fresh soil was sampled from the homogenized soils or from individual flasks and shaken for 2 hours with 42 ml ultrapure water on an orbital shaker (150 rpm). The slurries were filtered through 10 µm qualitative filter paper, pH of the extracts was measured on a MP-150 pH-meter (Mettler Toledo, Switzerland) and the extracts were frozen at -20 °C until further analyses. DOC and TN of the extracts and of the inocula (see section 3.3.1 for inocula preparation) were analysed on filtered and acidified aliquots (0.45 µm, Filtropur S, Sarstedt AG & Co., Germany; 50 µl 20% HCl to 20 ml filtrate) by high temperature catalytic oxidation using a Shimadzu TOC-V CPH analyser with a TN unit (Shimadzu Corporation, Japan). Ammonium and nitrate were measured from the water extracts on a AA3 system (SEAL Analytical Ltd, United Kingdom). Water extractable organic N was estimated by subtracting dissolved inorganic N (ammonia, nitrate and nitrite) from total water-extractable N. Soil moisture content (gravimetric) was determined by drying the soils at 105 °C for 48 h, and SOM by loss on ignition at 450 °C for 4 h. Soil physical and chemical variables prior to the beginning of the incubation for the four permafrost soils and the active layer soils used as inoculum are reported in Supplementary Table S1.

DNA extraction

Microcentrifuge tubes (1.5 ml) were filled with soil and snap-frozen in dry ice to analyse microbial communities from the flasks harvested after one day and at the end of the anoxic incubation. Initial soils were sampled likewise, after thawing and homogenizing but before pre-incubation for the permafrost soils and before preparing soil suspensions for active layer soils. The frozen tubes were kept at -80 °C for 4 to 17 months until freeze-drying, then homogenized by bead-beating (Precellys CK-68 15 ml tubes, Bertin Technologies, France, 2 × 30 s 5000 rpm). Between 100 and 300 mg of homogenized freeze-dried soil were used for DNA extraction using DNEasy PowerSoil Pro Kit

(Qiagen, Germany) according to the manufacturer's instructions, and DNA concentrations were measured on a Qubit (ThermoFisher, USA) 1.0 fluorometer.

Bacterial amplicon sequencing and bioinformatics

The V4-V5 region of the 16S ribosomal RNA gene was PCR amplified using primers 515F[37] and 926R[38] with Illumina sequencing adapters, in a 2-step PCR procedure with conditions described in Supplementary Table S2. For a subset of samples from the Cryoturbated soil, DNA concentrations were very low and thus the extracts were used undiluted and/or with 30 amplification cycles to obtain products. Each pool of 96 PCR products included samples, negative controls (1-3 replicates of each DNA extraction- and PCR-blank) and a mock community as positive control (2-5 replicates of ZymoBIOMICS Microbial Community DNA Standard, Zymo Research, USA). Two pools of 96 PCR products each were sequenced on Illumina MiSeq with V3 chemistry (2 × 300 bp, 15% PhiX spike-in) at the SNP&SEQ Technology Platform in Uppsala, where demultiplexing was performed by the sequencing platform.

Amplicon sequence variants (ASVs) were created in R 4.5.2 with *DADA2*[39] (pseudo-pooling) after removing non-target basepairs with *cutadapt*[40]. Taxonomy was assigned to ASVs with the RDP naïve Bayesian classifier[41] as implemented in *DADA2*, and ASVs resolved to the genus rank were further assigned a species rank by the exact string-matching algorithm implemented in *DADA2* (*assignSpecies*), with SILVA v138.1 reference data[42]. Putative contaminant ASVs were identified in silico using the *decontam* package[43]. The very low DNA concentrations in some DNA extracts, particularly so in the pre-incubation and day 1 extracts, would induce issues with the frequency-based method, therefore only the prevalence-based method was used to identify contaminants, with a threshold of 0.15 (more stringent than the default recommended value of 0.1). Contaminant status of the ASVs was evaluated separately for each sequencing flow cell, and subsequently combined using default parameters ('minimum'), leading to 26 contaminant ASVs amounting up to 0.18% of the overall 14.3 million good-quality reads. Further ASV filtering was carried out so that mock community positive controls would be depicted as accurately as possible: ASVs present in fewer than 3 samples or amounting up to fewer than 100 reads in total represented 8% of the reads and were removed. Samples with fewer than 20 000 reads were removed, resulting in a final ASV table of 13.1 million reads across 138 samples. Details of filtering steps, contaminant ASVs and intermediate files are found in the code and data repository.

Functional genes assays

To determine the genetic potential and potential bottleneck for different processes contributing to N_2O production and reduction, qPCR of several functional genes were performed: the ammonia-monooxygenase *amoA* found in betaproteobacterial ammonia oxidising bacteria[44] and ammonia

oxidising archaea[45] within the phylum Thermoproteota, nitrite-reductase genes in denitrification (*nirK*[46] and *nirS*[47]), and nitrous oxide-reductase genes (*nosZ* clades I[46] and II[48]), as well as the V4-V5 region of the bacterial 16S rRNA gene as a proxy for bacterial abundance[49]. DNA extracts were diluted to 1 ng μl^{-1} (or 1:8 for samples below 4 ng μl^{-1}). Two 15 µl reactions per gene were analysed on independent runs using CFX Connect or CFX-96 Real-Time System thermocyclers (Bio-Rad laboratories, USA), and primers and conditions described in Supplementary Table S2, with touchdown conditions for *nirS*, *nirK* and *nosZ* clade I. Each reaction contained 2 µl of diluted DNA template, 10 µg bovine serum albumin, 1x Biorad iQ™ SYBR®Green Supermix (Bio-Rad laboratories). The absence of polymerase inhibitors was ensured by amplifying a known amount of pCR 4-TOPO plasmid (Invitrogen, USA) added to the DNA extracts or no-template controls and comparing the threshold cycle number. No inhibition of the amplification reactions in any sample was detected with the amount of DNA used.

For samples where data was obtained for both *nir* and *nos* genes (Supplementary Table S3), we calculated the ratio of (*nirS* + *nirK*) / (*nosZ*I + *nosZ*II) as a proxy for potential N_2O source vs sink. Reliable quantitative data could not be obtained for bacterial *amoA* due to non-specific PCR amplification, and for the other genes, amplification could not always be obtained for all replicates (Supplementary Table S3). In the Cryoturbated soil, 16S rRNA gene copy numbers were orders of magnitude lower than for other soils, and only one sample (out of 24) yielded functional gene copy numbers above detection limits, and we therefore excluded Cryoturbated from further analyses and discussion of qPCR data.

Anoxic experiment

Permafrost and inocula preparation

The 'Palsa' permafrost was homogenized, decanted and set into flasks as described above but in an anaerobic glovebox under N_2 atmosphere. Soil moisture was measured using 5 g of homogenized soil (n = 4). Active layer soil suspensions were prepared using the active layer soil as described above, and compared a fresh soil inoculum (hereafter, 'Palsa') and an inoculum prepared with gamma-irradiated (45 kGy) soil as a negative control ('Control', see Supplementary Text for more detail).

Greenhouse gases measurements

Net CO_2, CH_4 and N_2O fluxes were measured and calculated as described above for CO_2, except for using an Agilent 7890 GC coupled with a flame ionization detector (FID, CO_2 and CH_4) and an electron capture detector (ECD, N_2O), and using moisturized N_2 instead of CO_2-free air for headspace flushing. N_2O remained below detection limit (100 ppb v:v) throughout the 175 days incubation. We estimated total warming potential by summing the mass of CO_2 and CH_4 converted into CO_2-*eq*. We

used the global warming potential at 100-year horizon for non-fossil CH_4 from IPCC (GWP_{100}, Table 7.15 in ref. [50]) as a conversion factor, that is multiplying grams of CH_4 by 27.0.

Statistical analyses

While the effects of inoculation on daily rate of aerobic CO_2 production were not necessarily stable through time, particularly in the first months (Supplementary Figure S1), we decided to avoid speculative interpretations of these patterns due to the lack of supporting data at this temporal resolution. We therefore focused on cumulative CO_2 production over the incubation and assessed how it was affected by inoculation treatments within each soil with one-way ANOVAs. Pairwise contrasts were computed when appropriate with the estimated marginal means method (*emmeans* package and function[51]) and Holm adjustment for multiple comparisons.

We measured N_2O at four dates and could therefore not calculate a cumulative budget for net N_2O production. Moreover, N_2O was below detection limit at most occasions, preventing statistical analyses except for the Palsa soil at day 7, where due to unequal sample sizes and variances we used a Kruskal-Wallis test on net N_2O fluxes, with inoculum as fixed factor.

Anaerobic CO_2 and CH_4 flux rates were analysed with repeated-measures ANOVA (RM-ANOVA with the *ezANOVA* package [52]), using time as within-subject variable and inoculum as between-subject variable. The time:inoculum interactions were not statistically significant ($P > 0.3$), therefore cumulative CO_2 and CH_4 over the incubation, as well as the product of their conversion into $CO_{2\text{-eq}}$ were compared between inoculum treatments using *t*-tests.

Differences in bacterial community composition between inoculation treatments for each soil type were assessed using *manyglm* models [53] separately for day 1 and day 389, and pairwise comparisons were obtained using Holm *P* value adjustment with the wrapper provided in the *mvabund* package [54].

Within each soil type, the effects of the different inoculation treatments on most variables (functional gene abundances, TOC, TN, organic matter content, moisture, pH) were assessed with one-way ANOVAs using inoculation as a fixed factor, followed by pairwise contrasts when appropriate, using log-transformed data when necessary to meet ANOVA assumptions or Kruskal-Wallis tests when assumptions were not met (Supplementary Table S4). Since our hypotheses focused on treatment effects rather than temporal dynamics *per se*, separate ANOVAs were carried out one day after inoculation – to test for putative artefacts introduced by inoculation – and at the end of the incubation to test for functional consequences of inoculation.

Results

Soil chemistry

Changes in soil chemistry upon inoculation could obfuscate impacts of microbial community dynamics, thus we assessed whether soil chemistry variables were affected one day after inoculation. Soil moisture was unaffected by inoculation treatments, while other factors were, although mainly in the Palsa soil. Here, soil pH was affected by inoculation with increased pH for the positive control and active layer inoculum compared to the negative control, by 0.68 and 0.90, respectively, (± 0.23, t = 2.90 and 3.85, P = 0.042 and 0.010, respectively, df = 9). Likewise, total dissolved N, ammonium, and dissolved inorganic N were slightly lower after inoculum addition in the Palsa soil. There were small decreases in water-extractable DOC in two inoculated soils relative to the control (Tussock and Palsa P = 0.010 and 0.003, respectively), and a small decrease in DON in Tussock soil but only when inoculated with its own active layer (Supplementary Figure S2). Nitrate and nitrite were undetected at day 1, except in some Tussock soils and in samples inoculated with the positive control. We further explored putative artefacts due to chemistry alteration upon inoculation in Supplementary Text.

At the end of the oxic incubation, day 389, dissolved inorganic N was significantly higher in the positive control inoculum treatments, in both Cryoturbated soil and Tussock peat (Supplementary Table S4, Supplementary Figure S2); inorganic N pools are further discussed below in relation to N_2O fluxes. Water-extractable total dissolved N had increased up to 9-fold compared to the start of the incubation, with water-extractable organic N increasing 2 to 9-fold (Supplementary Figure S3), irrespective of inoculation. Dissolved organic C content decreased significantly for the positive control in Yedoma sediment. Other soil variables (SOM content, pH, moisture, total and organic N) were unaffected by inoculation treatments, with the exception of inorganic N pools discussed further down.

Greenhouse gas production

Aerobic CO_2 production

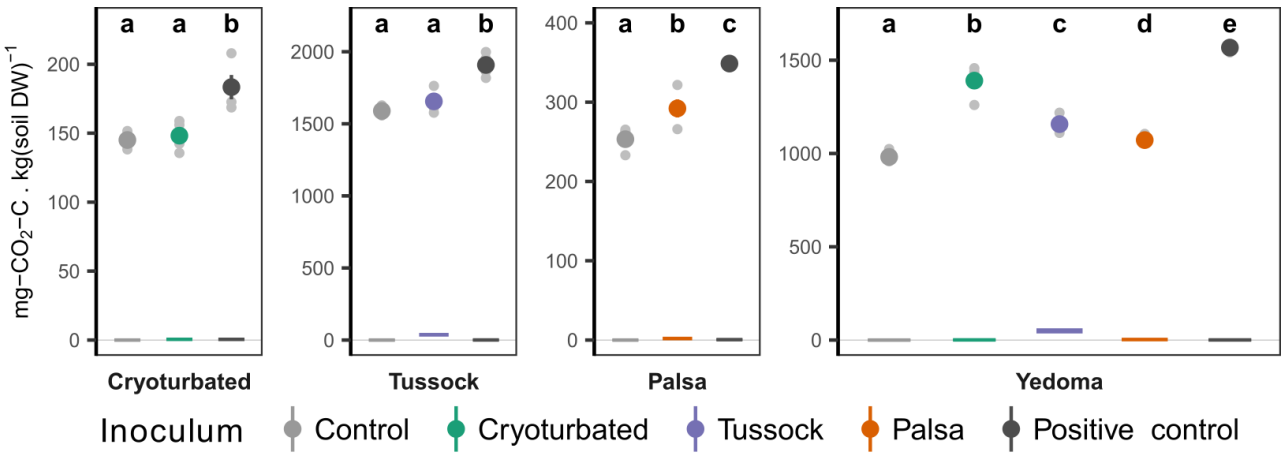

Figure 2: Cumulative CO_2 production of four permafrost soils subjected to microbial community manipulation after 389 days of oxic incubation. Large symbols and error-bars indicate mean +/- SE (n=4), small grey dots are individual measurements. Horizontal bars denote the amount of carbon introduced by the inoculum solutions. Letters denote significant (Holm-adjusted $P < 0.05$) differences between inoculum treatments within a given soil type.

We found clear limitations of CO_2 production in all soils. The positive control inoculum (addition of a functionally diverse community) enhanced the production of CO_2 in all soils, with increases in cumulative CO_2 production ranging from 20.1 to 59.6 % (Figure 2). CO_2 production in the Palsa permafrost increased significantly in response to its own active layer inoculation (+15.4 %, 95% CI 8.3–22.5 %, $t = 3.47$, df = 9, $P = 0.007$), while neither the Tussock nor Cryoturbated soil responded when inoculated with their respective active layer community. For the Yedoma deposit, all three active layer inoculums significantly increased CO_2 production, but to a lesser extent than the positive control. Further, the order was reversed, with Cryoturbated active layer inoculum causing the greatest increase (41.5 %, CI 36.2–46.6 %, $t = 11.58$, $P < 0.001$; df = 15), Tussock intermediate (17.8 %, CI 12.4–23.2 %, $t = 4.98$, $P = 0.001$), and Palsa the smallest (9.1 %, CI 3.7–14.1 %, $t = 2.55$, $P = 0.044$, Figure 2).

Aerobic N_2O production

Inorganic N dynamics and N_2O production provide further indication of functional limitations, as they strongly responded to inoculation, mainly by the positive control. At the end of the incubation, ammonium had decreased in all soils regardless of inoculation, by 60-100% (Figure 3a). Very high nitrate and nitrite content, in some cases far exceeding initial ammonium concentrations, were observed in soils inoculated with the positive control, except for the Palsa soil where nitrate was no longer detected (Figure 3b).

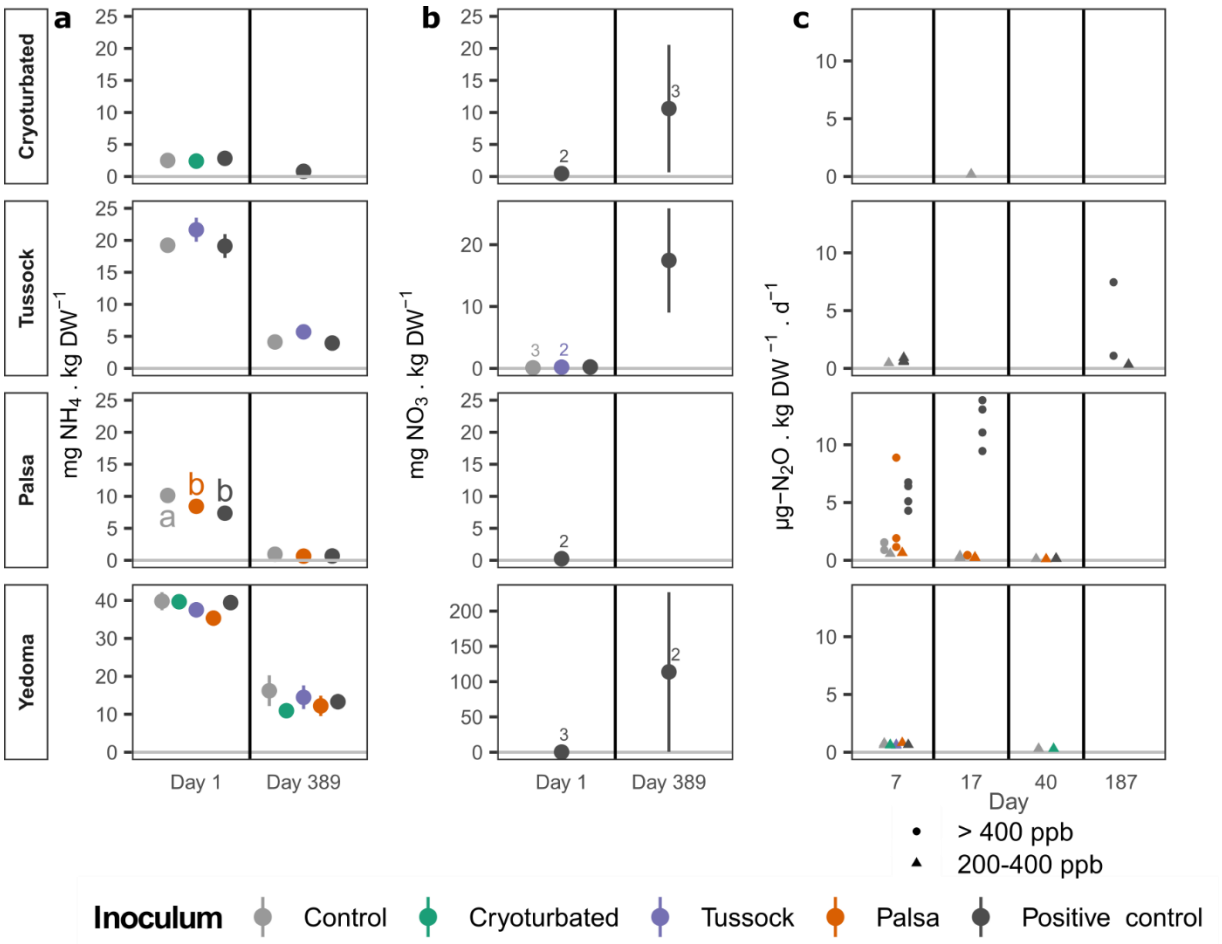

Figure 3: Water-extractable dissolved inorganic nitrogen pools ammonium (a) and nitrate+nitrite (b), and net N_2O flux rates (c) in four permafrost soils subjected to microbial community manipulation over 389 days of oxic incubation.
Symbols in **(a)** and **(b)** indicate mean +/- SE, (n = 4 unless indicated otherwise by numbers when below detection limit), different letters denote statistically significant differences ($P < 0.05$). Small symbols in **(c)** represent individual measurements, triangles denote trace amounts shown and discussed but excluded from statistical analyses, measurement values below 200 ppb (0.5×detection limit) are not shown.

In the Palsa soil, net N_2O emissions were initially (day 7) higher in the positive control than in the negative control or the active layer inoculum (Figure 3), with a +425% increase in the positive control compared to the negative control (Figure 3; negative control: mean ± SE 1.32 ± 0.37 µg N_2O-N day^{-1} $kg\ dry\ soil^{-1}$ and 95%CI 0.60–2.05, n = 3; positive control mean ± SE 5.65 ± 1.15 CI: 3.39–7.90, n = 4). However, the measurements below detection limit and non-parametric approach make this strong increase not statistically significant (Kruskal-Wallis $X^2 = 4.3$, df = 2, $P = 0.112$). After 17 days, N_2O was detected in the active layer treatment (n = 2, mean ± SE: 0.45 ± 0.02 µg-N_2O-N day^{-1} $kg\ dry\ soil^{-1}$) and several orders of magnitude higher in the positive control (n = 4, mean ± SE: 11.86 ± 0.99 µg-N_2O-N day^{-1} $kg\ dry\ soil^{-1}$) – this increase was not statistically tested due to low sample size. N_2O was further found in trace amounts (200–400 ppb) in the negative control and active layer treatment (n = 4 and 2, respectively). N_2O was only observed in trace amounts at day 40 and was below the detection limit at day 187 (400 ppb equivalent c 0.4–1.4 µg N_2O-N kg soil $DW^{-1}d^{-1}$ over days 180-187). *In the Tussock soil*, N_2O was detected in trace amounts at day 7 in the negative and

positive controls (in 1 and 4 replicates, respectively), then at day 187 in large amounts in the positive control inoculum treatment only (n = 2). In the Cryoturbated and Yedoma soils, nitrous oxide remained below detection limit in all treatments at all time points, and was only occasionally detected in trace amounts.

Anaerobic greenhouse gas production in Palsa

Methane production was clearly limited in the Palsa soil which was incubated under anoxic conditions. Methane production increased in Palsa permafrost inoculated with its own active layer compared to the negative control (RM-ANOVA $F_{8,84} = 61.22$, Greenhouse-Geisser ε corrected-$P < 0.001$), resulting in a quintupling of cumulative CH_4 production over six months (Figure 4b; +395 %, CI 339–452 %, $t = 10.51$, df = 21, $P < 0.001$), while CO_2 production significantly decreased (W = 56, $P = 0.01$, df = 15, Figure 4a), and N_2O was not detected. Cumulative estimated warming potential (using GWP_{100} for non-fossil CH_4 as conversion factor) increased by 35% with inoculation (CI 15–59%, $t = 8.27$, $P = 0.003$, Figure 4c).

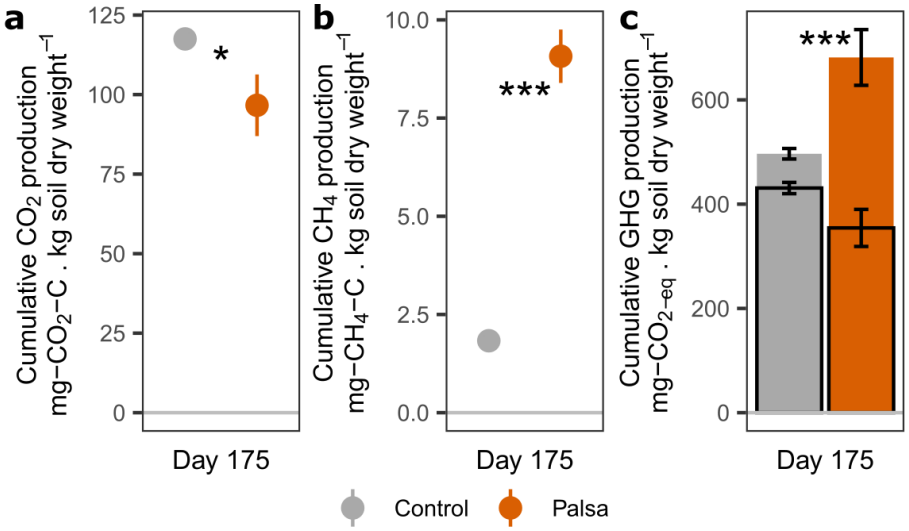

Figure 4: Cumulative CO_2 (a), CH_4 (b) and $CO_{2\text{-eq}}$ (c) production of Palsa permafrost subjected to microbial community manipulation over 175 days of anoxic incubation.
Symbols and error-bars indicate mean +/- SE (n=8). Coloured bars in (**c**) indicate $CO_{2\text{-eq}}$, black outline bars denote the CO_2 fraction of $CO_{2\text{-eq}}$ (data from **a** converted from mg-CO_2-C to mg-CO_2). Symbols denote statistically significant differences (**a**: Wilcoxon rank sum exact test, **b-c**: *t*-test with unequal variances, ***: $P < 0.001$; *: $P < 0.05$).

Bacterial dynamics in oxic incubation

Community-level initial soil differences and inoculation effects

Bacterial community coalescence and increased bacterial richness were observed in some inoculation treatments. These changes coincided with biogeochemical changes described in previous sections.

Before the incubation, the bacterial communities in the different active layers and positive control soils differed significantly from each other (*manyglm* pairwise comparisons $P = 0.018$, n = 4). The bacterial communities in permafrost soils prior to incubation also appeared to differ from each other and from active layer soils, although this could not be formally tested as too few replicates passed quality filtering (Supplementary Figure S4).

One day after inoculation the composition of the bacterial communities were only affected by inoculation of the positive control in the Tussock and Palsa permafrost soils (Figure 5). Tussock and Yedoma soils also showed an increase in bacterial richness in the positive control, and in the Palsa soil with both the active layer inoculum and positive control (Figure 5). Bacterial abundance, estimated by the number of 16S rRNA gene copies, was initially unaffected by inoculation, except for the Palsa soil where the positive control was one order of magnitude higher than the negative control or the active layer inoculum (respectively $t = 3.19$ and 2.66, $P = 0.033$ and 0.052, df = 9, Figure 6).

After 389 days of incubation, bacterial community composition in all inoculation treatments differed significantly from each other and the negative control in the Palsa and Yedoma permafrost (*manyglm* post-hoc pairwise comparisons $P < 0.05$, Supplementary Table S5, Figure 5). In the Tussock soil, the positive control differed from the negative control, but the active layer inoculum treatment did not, while in the Cryoturbated soil no significant differences were observed between treatments. Bacterial richness estimates corresponded to changes in community composition, with significant increases in estimated richness only in cases where communities significantly differed from the negative control. Bacterial biomass was 1-3 orders of magnitude higher at the end than at the beginning of the incubation, regardless of inoculation treatments, except for the Yedoma sediment where the positive control was one order of magnitude below the negative control and Palsa inoculum ($t > 3.11$, $P < 0.02$, df = 15, Figure 6).

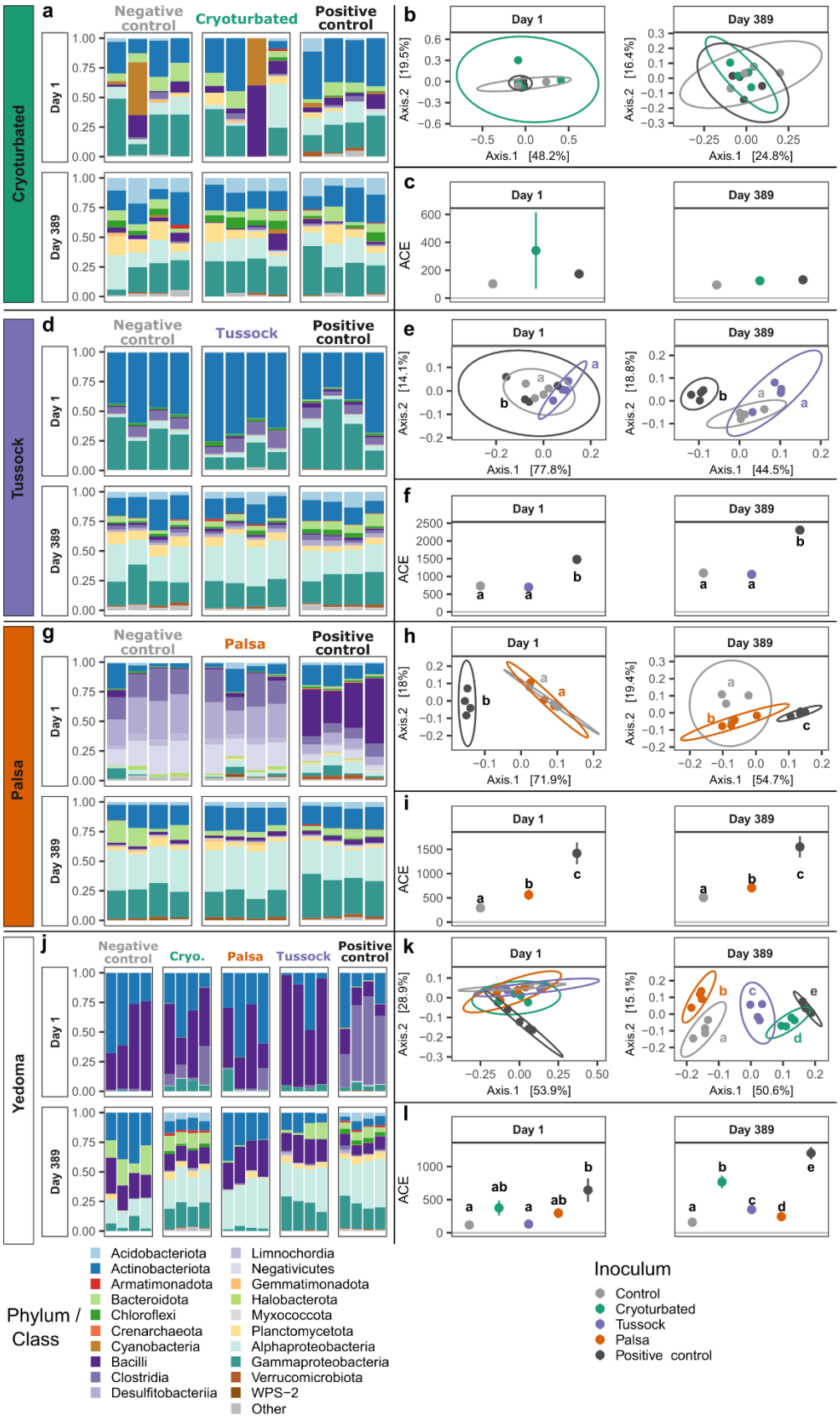

Figure 5: Bacterial community composition (16S V4V5 amplicons) in four permafrost soils subjected to microbial community manipulation over 389 days of oxic incubation.
a,d,g,j: Relative abundance of the 20 most abundant bacterial phyla (class for Firmicutes and Proteobacteria), each stack of bars represents one sample.
b,e,h,k: Principal coordinate analyses (PCoA) of weighted UniFrac distances. Points represent individual samples, ellipses indicate 95% confidence intervals for each treatment (n=4). Different lower-case letters indicate significant differences within a soil-date combination (manyglm pairwise comparison $P < 0.05$).
c,f,i,l: Species richness estimate (abundance-based coverage estimator ACE). Symbols and error-bars represent means +/- SE (n=4), different letters indicate significant differences between inoculums within a soil-date combination (EMmeans Holm-adjusted $P < 0.05$).

Functional genes

Archaeal *amoA* genes supporting ammonia oxidation in the nitrification process were prevalent in the Cryoturbated active layer soil, but were otherwise in low abundance (100–400 copies per g dry soil) or below detection at day 1, but not detected at day 389 unless inoculated with the positive control (Figure 6). Bacterial *amoA* genes were not detected. By contrast, *nir* and *nosZ* genes were detected in all soils by the end of the incubation, regardless of inoculation, even though they were either low in abundance or not detected on day 1 (Figure 6). As a proxy for N_2O source vs sink potential, the *nir* / *nos* ratio was largely unaffected by inoculation (Supplementary Figure S5), although there was a significant increase in Tussock soil, with the positive control being the only treatment with a *nir* / *nos* ratio higher than 1, suggesting a stronger source than sink potential. In the Palsa soil, the active layer and positive control inoculum had significantly different *nir*/*nos* ratios, suggesting a sink in the active layer and a source in the positive control. However, neither differed from the negative control. Minute amounts of ribosomal and functional genes were detected in the Cryoturbated permafrost soil overall and therefore not interpreted further.

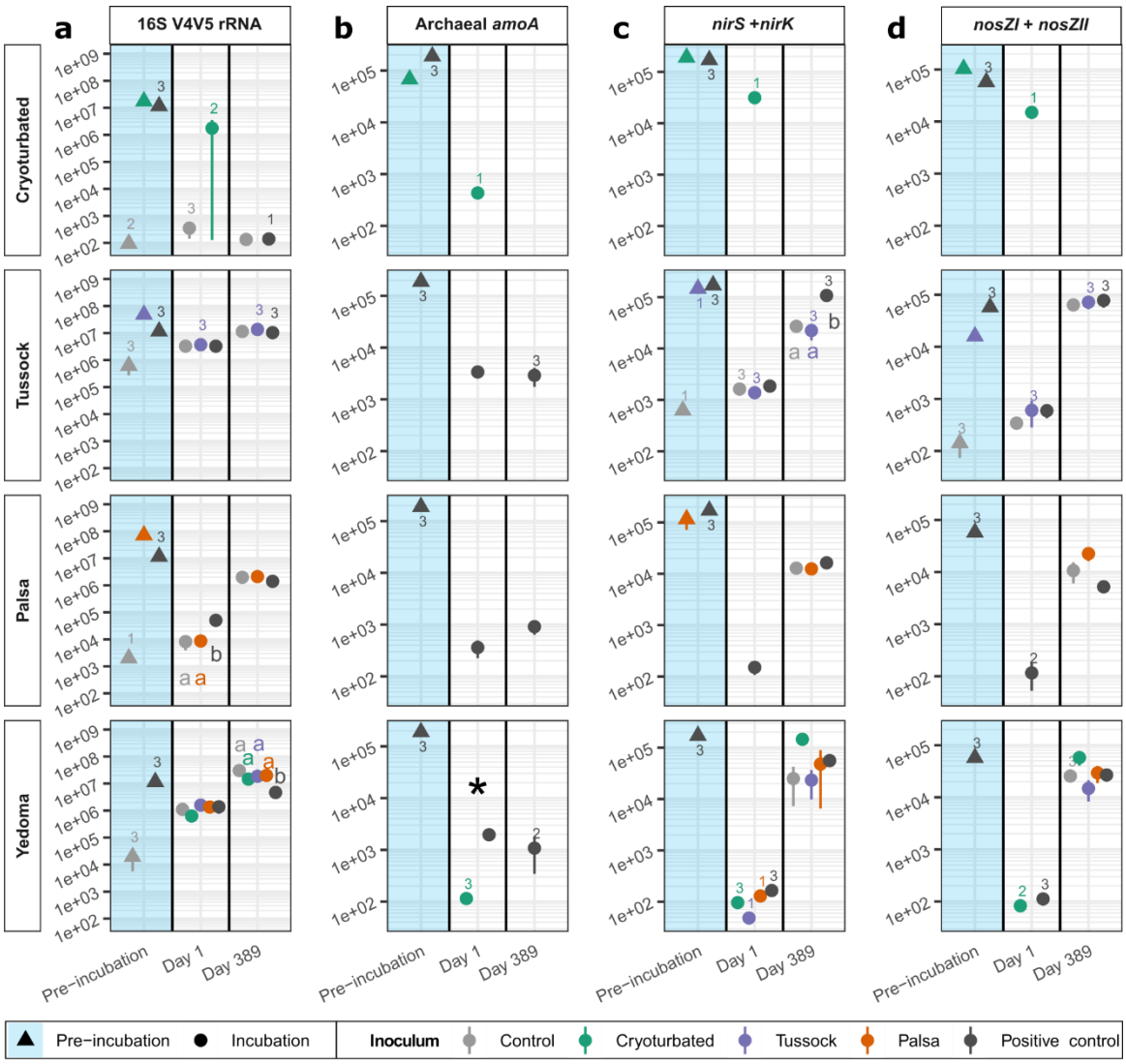

Figure 6: Abundance of ribosomal gene (a) and genes controlling nitrification (b), production (c) and consumption (d) of N_2O in four permafrost soils subjected to microbial community manipulation over 389 days of oxic incubation.
Gene copy number per g soil dry weight. Symbols and error-bars indicate mean +/- SE (n=4 unless indicated otherwise by numbers when below detection limit), letters indicate statistically significant differences within a soil:date combination (EMmeans Holm-adjusted $P < 0.05$), asterisk denotes significant differences within a soil:date combination (*t*-test $P < 0.05$). Pre-incubation samples are the respective permafrost soils prior to incubation (Control), active layer (Turbel, Palsa, Tussock) and positive control soils used for inoculum suspensions.

Discussion

Functional limitations were observed in all permafrost soils, as evidenced by large increases in CO_2 production (20–60%, Figure 2), changes in inorganic N pools (Figure 3) and introduction of missing N-cycling genes (Figure 6) when inoculated with the functionally-diverse positive control. In addition, we found indications of functional limitation of N_2O and of CH_4 production in some of the permafrost soils. Our hypothesis that changes in biogeochemistry would correspond to changes in bacterial community composition, was largely supported: changes in dynamics of GHG production or inorganic N pools were only detected in cases where bacterial community composition was significantly modified by inoculation, with the exception of the Cryoturbated soil where DNA-based results are suboptimal. Strong and long-lasting changes in community composition, systematically

linked to an increase in bacterial richness, indicate that coalescence events[55,56] occurred between permafrost and inoculum communities (Figures 2 and 5). The framework of microbial functional limitations of biogeochemical processes in permafrost, hitherto only shown in Pleistocene-old Yedoma deposits[9–11] is therefore relevant across all common types of permafrost, even in more recent Holocene deposits. This suggests that functions can be missing or lost from permafrost microbial communities not only in permafrost frozen for dozens of millennia[25] but also over time scales of a few centuries to a few thousand years.

Microbial communities from local active layers were not consistently able to alleviate the functional limitations to the same extent as our positive control. This could be because the microbial communities in the active layers were missing the same functions as those in the underlying permafrost layers, which agrees with the selected N-cycling functional genes not always being observed in the active layer soils we used for inoculation (Figure 6). This corroborates observations of truncated denitrifier communities in topsoils notably in the tundra[31,57], but it is unclear how common this is over space and soil depth throughout the Arctic. *nir* and *nosZ* genes in denitrifiers were likely present from the beginning in amounts below the detection limit of our qPCR assays, in both the active layer inoculums and permafrost soils: indeed, *nir* and *nosZ* gene copy numbers within a given soil were similar in abundance by the end of the incubation regardless of inoculation. Thus, the active layer samples we used for inoculation were likely missing some functions, but not all. Another explanation is that microbial communities in active layer soils carried the functions missing from the permafrost, but failed to establish in the permafrost and introduce these missing functions. Indeed, successful coalescence events appear as a necessary condition to the restoration of missing functions. All permafrost soils were susceptible to coalescence at least with the positive control (with the exception of the Cryoturbated soil, where the DNA-based results are suboptimal), and all active layer inocula induced coalescence in the Yedoma sediment (Figure 5), ruling out bacterial communities in the inocula being unable to establish in permafrost soil. Our experiments were not designed to answer which drivers favour or impede microbial community coalescence in newly-thawed permafrost, but our ancillary measurements offer insights. Differences in pH, organic matter content or DOC between permafrost and active layer did not provide consistent explanations for the (lack of) success of coalescence (Supplementary Figure S2). Therefore, this suggests that the success of coalescence could depend on host- or guest- soil community or soil variables beyond our range of measurements. While the factors affecting modalities and consequences of microbial community assembly upon thaw are increasingly studied[12,17,21,58], combinations of field and laboratory experiments distributed across the permafrost region will be critical to assess the (lack of)

functionality of active layer microbial communities, the controls over coalescence dynamics and their biogeochemical implications.

The Palsa inoculum, which was the only one to induce a significant increase in CO_2 production in its own permafrost, induced the lowest increase in Yedoma permafrost. Conversely, the Cryoturbated inoculum, which did not increase CO_2 production in Cryoturbated permafrost, induced the highest increase in Yedoma This suggests that the impact of coalescence events is thus far difficult to predict, but may depend on the complementarity between functions present in the permafrost and active layer, as well as on microbial factors determining the success of coalescence. We speculate that certain functions may be entirely missing in both active and permafrost layers, but that those functions differ across soil types or space. Under this assumption, microbial dispersal through percolation upon active layer deepening may not efficiently restore the limited functional potential of permafrost microbial communities. More disruptive permafrost thaw events involving soil mixing, such as thaw slumps or thermokarst features, may have greater impacts on microbial communities as additional vectors of dispersal, such as wind[59,60] or soil fauna[61] could then accelerate microorganism migration into newly-thawed permafrost. Increasing anthropic pressure in the Arctic, notably through tourism and mining, may also increase microbial dispersal[62] which could harmonize the functionality of active layer microbial communities. Understanding the variability of active layer microbial communities and of their potential to alleviate permafrost functional limitations is essential to assess the feasibility and impact of measures mitigating microbial dispersal.

Nitrous oxide production in oxic incubation was increased in Palsa soil when inoculated with both the active layer inoculum and the positive control, and in the Tussock soil, N_2O production was only detected in the positive control. The rates of net N_2O production (0.44–13.86 µg N_2O-N kg DW^{-1} d^{-1}) are within the range of those in the literature (Supplementary Table S6, [11,63–69]) under similar settings, i.e. oxic conditions without plants. The processes governing N_2O production are therefore affected by functional limitations in these two soils, and not only in Yedoma soils as previously observed[11]. However, the abundance of genes indicating the capacity for production of N_2O from NO_2^- and NO_3^- (*nirK* and *nirS*) and the reduction of N_2O into N_2 (*nosZI* and *nosZII*)[70] in the denitrification pathway did not differ between treatments. Together with the introduction of archaeal *amoA* genes by the positive control, and the observation of nitrate only where *amoA* genes were introduced, this suggests that the observed functional limitations of net N_2O production is linked to a limited oxidation process of NH_4^+ to NO_3^- (nitrification process). Ammonia oxidizing bacteria are known to produce more N_2O than the archaeal counterpart[71], yet bacterial *amoA* genes could not be quantified and only archaeal *amoA* genes were introduced with the positive control. Nevertheless, the primers used for bacterial *amoA* quantification do not target *amoA* in complete nitrifying bacteria,

which have an oligotrophic lifestyle[72] and were recently shown to be abundant in Arctic soils[73]. Based on the bacterial sequences, they were, however, only observed in two samples that were not inoculated with the positive control, although our 16S rRNA gene primers may not have detected all complete nitrifiers within the genus *Nitrospira*[74]. Contrary to our previous findings[10], ammonium content decreased in all soils throughout the incubation, regardless of inoculation, which we therefore cannot entirely attribute to ammonia oxidation. Since microbial biomass increased by 1-2 orders of magnitude during the incubation the decrease can also be explained by assimilation of ammonium into microbial biomass. Further, complete denitrification to N_2 may have occurred before we could detect nitrate or N_2O. Thus, unclear N dynamics remain at play, notably an ubiquitous and large increase in organic N over the incubation, in all soils regardless of inoculation. Our results suggest microbial community composition can be a determining factor in the variability of net N_2O production.

We found a strong functional limitation of methanogenesis under anoxic conditions, evidenced as a quintupling of cumulative CH_4 production in the presence of active layer inoculum. This was not balanced by the decrease in CO_2 production, and in $CO_{2\text{-eq}}$ this resulted in a 35% increase in GHG emissions over six months. Functional limitations of methanogenesis were originally observed in Pleistocene-old Yedoma permafrost, where CH_4 production only occurred in isolated permafrost samples in a multi-year incubation, but could be restored by cross-inoculation from other samples where this function was present[9]. Our results expand upon these earlier observations: in our more recent Holocene permafrost deposits (SOM dated to c. 9100 yrs BP[75,76]) that had presumably been perennially frozen for a shorter time, methanogenesis occurred consistently in all eight control replicates, but its rate quintupled after introduction of active layer microorganisms. The earlier observations suggested an on-off switch in methanogenesis triggered by the presence/absence of methanogens[9], but our results instead suggest that even permafrost in which CH_4 production is observed can produce CH_4 at much higher rates upon introduction of methanogen communities present in the active layer. This is in line with the correlation observed between net CH_4 fluxes and abundances of Candidatus *Methanoflorens stordalenmirensis* in the active layer of newly-thawed permafrost from a neighbouring peatland[77]. Our results highlight that when estimating CH_4 production from permafrost based on incubations, it is necessary to account for the increased functional potential upon coalescence with active layer microbial communities.

To conclude, we demonstrate microbial functional limitations of the three major biogenic greenhouse gases CO_2, N_2O and CH_4 across three Holocene permafrost soils as well as in the older Yedoma deposits. Active layer microbial communities could not always entirely alleviate these functional limitations, which we attribute to unsuccessful community coalescence, and when they could, they

were outperformed by temperate soil microorganisms, probably due to active layer microbial communities missing functions. Upon coalescence with topsoil microorganisms, we observed increases in CO_2 production of up to 60%, and for N_2O and CH_4 up to 400%. The consequences on the arctic terrestrial carbon-climate feedback could therefore be globally relevant. We propose that it is crucial to rapidly assess (a) the spatial variability in the functional potential of active layer microbial communities and how this might change in a warmer Arctic, (b) the conditions under which coalescence is possible or impeded, and (c) how other soil biota such as roots, fauna or humans may mediate coalescence. We recommend combining the functional assessment of a collection of circum-Arctic soil samples with mechanistic laboratory and in situ studies untangling the drivers of community coalescence to bridge these knowledge gaps. Such knowledge will be required to elaborate strategies limiting microbial dispersal under increasing anthropic pressure in the Arctic, to predict these expected large increases in biogenic GHG production and account for those in climate change mitigation scenarios.

Data and code availability

All data and code used to produce the findings presented in this study are available at https://doi.org/10.57669/monteux-2026-permafrost-inoculation-1.0.0 / https://git.bolin.su.se/bolin/monteux-2026-permafrost-inoculation/-/releases/1.0.0

Sequencing data is available at ENA under project accession number PRJEB97802.

References

1. Hugelius, G. *et al.* Estimated stocks of circumpolar permafrost carbon with quantified uncertainty ranges and identified data gaps. *Biogeosciences* **11**, 6573–6593 (2014).
2. Schuur, E. A. G. *et al.* Climate change and the permafrost carbon feedback. *Nature* **520**, 171–179 (2015).
3. Natali, S. M. *et al.* Permafrost carbon feedbacks threaten global climate goals. *Proceedings of the National Academy of Sciences* **118**, e2100163118 (2021).
4. Schädel, C. *et al.* Earth system models must include permafrost carbon processes. *Nat. Clim. Chang.* 1–3 (2024) doi:10.1038/s41558-023-01909-9.
5. Schädel, C. *et al.* Potential carbon emissions dominated by carbon dioxide from thawed permafrost soils. *Nature Clim. Change* **6**, 950–953 (2016).

6. Schädel, C. *et al.* Circumpolar assessment of permafrost C quality and its vulnerability over time using long-term incubation data. *Glob Change Biol* **20**, 641–652 (2014).
7. Koven, C. D. *et al.* A simplified, data-constrained approach to estimate the permafrost carbon–climate feedback. *Philosophical Transactions of the Royal Society A: Mathematical, Physical and Engineering Sciences* **373**, 20140423 (2015).
8. McGuire, A. D. *et al.* Dependence of the evolution of carbon dynamics in the northern permafrost region on the trajectory of climate change. *PNAS* **115**, 3882–3887 (2018).
9. Knoblauch, C., Beer, C., Liebner, S., Grigoriev, M. N. & Pfeiffer, E.-M. Methane production as key to the greenhouse gas budget of thawing permafrost. *Nature Climate Change* **8**, 309–312 (2018).
10. Monteux, S. *et al.* Carbon and nitrogen cycling in Yedoma permafrost controlled by microbial functional limitations. *Nature Geoscience* **13**, 794–798 (2020).
11. Marushchak, M. E. *et al.* Thawing Yedoma permafrost is a neglected nitrous oxide source. *Nat Commun* **12**, 7107 (2021).
12. Ernakovich, J. G. *et al.* Microbiome assembly in thawing permafrost and its feedbacks to climate. *Global Change Biology* **28**, 5007–5026 (2022).
13. Monteux, S. *et al.* Long-term in situ permafrost thaw effects on bacterial communities and potential aerobic respiration. *The ISME Journal* **12**, 2129–2141 (2018).
14. Johnston, E. R. *et al.* Responses of tundra soil microbial communities to half a decade of experimental warming at two critical depths. *PNAS* **116**, 15096–15105 (2019).
15. Mackelprang, R. *et al.* Metagenomic analysis of a permafrost microbial community reveals a rapid response to thaw. *Nature* **480**, 368–371 (2011).
16. Barbato, R. A. *et al.* Not all permafrost microbiomes are created equal: Influence of permafrost thaw on the soil microbiome in a laboratory incubation study. *Soil Biology and Biochemistry* 108605 (2022) doi:10.1016/j.soilbio.2022.108605.
17. Doherty, S. J., Thurston, A. K. & Barbato, R. A. Active layer and permafrost microbial community coalescence increases soil activity and diversity in mixed communities compared to permafrost alone. *Front. Microbiol.* **16**, (2025).
18. Bottos, E. M. *et al.* Dispersal limitation and thermodynamic constraints govern spatial structure of permafrost microbial communities. *FEMS Microbiol Ecol* **94**, fiy110 (2018).

19. Fontaine, S. *et al.* Plant–soil synchrony in nutrient cycles: Learning from ecosystems to design sustainable agrosystems. *Global Change Biology* **30**, e17034 (2024).
20. Jones, C. M. *et al.* Recently identified microbial guild mediates soil N2O sink capacity. *Nature Clim Change* **4**, 801–805 (2014).
21. Starr, S. F. *et al.* Organic Matter Composition Versus Microbial Source: Controls on Carbon Loss From Fen Wetland and Permafrost Soils. *Journal of Geophysical Research: Biogeosciences* **130**, e2024JG008445 (2025).
22. Strauss, J. *et al.* Organic matter storage and vulnerability in the permafrost domain. in *Encyclopedia of Quaternary Science* 399–410 (Elsevier, 2025). doi:10.1016/B978-0-323-99931-1.00164-1.
23. Schirrmeister, L. *et al.* Yedoma: Late Pleistocene ice-rich syngenetic permafrost of Beringia. in *Encyclopedia of Quaternary Science* 296–311 (Elsevier, 2025). doi:10.1016/B978-0-323-99931-1.00223-3.
24. Strauss, J. *et al.* A globally relevant stock of soil nitrogen in the Yedoma permafrost domain. *Nat Commun* **13**, 6074 (2022).
25. Caro, T. A. *et al.* Microbial Resuscitation and Growth Rates in Deep Permafrost: Lipid Stable Isotope Probing Results From the Permafrost Research Tunnel in Fox, Alaska. *Journal of Geophysical Research: Biogeosciences* **130**, e2025JG008759 (2025).
26. Hugelius, G. *et al.* Large stocks of peatland carbon and nitrogen are vulnerable to permafrost thaw. *PNAS* **117**, 20438–20446 (2020).
27. Leppiniemi, O., Karjalainen, O., Aalto, J., Luoto, M. & Hjort, J. Environmental spaces for palsas and peat plateaus are disappearing at a circumpolar scale. *The Cryosphere* **17**, 3157–3176 (2023).
28. Fewster, R. E. *et al.* Imminent loss of climate space for permafrost peatlands in Europe and Western Siberia. *Nat. Clim. Chang.* 1–7 (2022) doi:10.1038/s41558-022-01296-7.
29. Hamard, S. *et al.* Microbial photosynthesis mitigates carbon loss from northern peatlands under warming. *Nat. Clim. Chang.* **15**, 436–443 (2025).
30. Väisänen, M., Krab, E. J. & Dorrepaal, E. Carbon dynamics at frost-patterned tundra driven by long-term vegetation change rather than by short-term non-growing season warming. *Biogeochemistry* **136**, 103–117 (2017).
31. Pessi, I. S. *et al.* In-depth characterization of denitrifier communities across different soil ecosystems in the tundra. *Environmental Microbiome* **17**, 30 (2022).

659 32. Väisänen, M. *et al.* Meshes in mesocosms control solute and biota exchange in soils: A step towards
660 disentangling (a)biotic impacts on the fate of thawing permafrost. *Applied Soil Ecology* **151**, 103537
661 (2020).
662 33. Wertz, S. *et al.* Maintenance of soil functioning following erosion of microbial diversity. *Environmental*
663 *Microbiology* **8**, 2162–2169 (2006).
664 34. Fontaine, S. *et al.* Stability of organic carbon in deep soil layers controlled by fresh carbon supply.
665 *Nature* **450**, 277–280 (2007).
666 35. Fontaine, S. *et al.* Fungi mediate long term sequestration of carbon and nitrogen in soil through their
667 priming effect. *Soil Biology and Biochemistry* **43**, 86–96 (2011).
668 36. D'Amico, S. *et al.* Psychrophilic microorganisms: challenges for life. *EMBO reports* **7**, 385–389 (2006).
669 37. Parada, A. E., Needham, D. M. & Fuhrman, J. A. Every base matters: assessing small subunit rRNA
670 primers for marine microbiomes with mock communities, time series and global field samples.
671 *Environmental Microbiology* **18**, 1403–1414 (2016).
672 38. Quince, C., Lanzen, A., Davenport, R. J. & Turnbaugh, P. J. Removing Noise From Pyrosequenced
673 Amplicons. *BMC Bioinformatics* **12**, 38 (2011).
674 39. Callahan, B. J. *et al.* DADA2: High-resolution sample inference from Illumina amplicon data. *Nat*
675 *Methods* **13**, 581–583 (2016).
676 40. Martin, M. Cutadapt removes adapter sequences from high-throughput sequencing reads.
677 *EMBnet.journal* **17**, 10–12 (2011).
678 41. Wang, Q., Garrity, G. M., Tiedje, J. M. & Cole, J. R. Naive Bayesian Classifier for Rapid Assignment of
679 rRNA Sequences into the New Bacterial Taxonomy. *Applied and Environmental Microbiology* **73**,
680 5261–5267 (2007).
681 42. Quast, C. *et al.* The SILVA ribosomal RNA gene database project: improved data processing and web-
682 based tools. *Nucleic Acids Res* **41**, D590-596 (2013).
683 43. Davis, N. M., Proctor, D. M., Holmes, S. P., Relman, D. A. & Callahan, B. J. Simple statistical
684 identification and removal of contaminant sequences in marker-gene and metagenomics data.
685 *Microbiome* **6**, 226 (2018).
686 44. Rotthauwe, J. H., Witzel, K. P. & Liesack, W. The ammonia monooxygenase structural gene amoA as a
687 functional marker: molecular fine-scale analysis of natural ammonia-oxidizing populations. *Appl.*
688 *Environ. Microbiol.* **63**, 4704–4712 (1997).

689 45. Tourna, M., Freitag, T. E., Nicol, G. W. & Prosser, J. I. Growth, activity and temperature responses of
690 ammonia-oxidizing archaea and bacteria in soil microcosms. *Environmental Microbiology* **10**, 1357–
691 1364 (2008).
692 46. Henry, S., Bru, D., Stres, B., Hallet, S. & Philippot, L. Quantitative detection of the nosZ gene, encoding
693 nitrous oxide reductase, and comparison of the abundances of 16S rRNA, narG, nirK, and nosZ genes in
694 soils. *Appl Environ Microbiol* **72**, 5181–5189 (2006).
695 47. Throbäck, I. N., Enwall, K., Jarvis, Å. & Hallin, S. Reassessing PCR primers targeting nirS, nirK and
696 nosZ genes for community surveys of denitrifying bacteria with DGGE. *FEMS Microbiology Ecology*
697 **49**, 401–417 (2004).
698 48. Jones, C. M., Graf, D. R., Bru, D., Philippot, L. & Hallin, S. The unaccounted yet abundant nitrous
699 oxide-reducing microbial community: a potential nitrous oxide sink. *ISME J* **7**, 417–426 (2013).
700 49. Muyzer, G., Waal, E. C. de & Uitterlinden, A. G. Profiling of complex microbial populations by
701 denaturing gradient gel electrophoresis analysis of polymerase chain reaction-amplified genes coding for
702 16S rRNA. *Appl. Environ. Microbiol.* **59**, 695–700 (1993).
703 50. Intergovernmental Panel on Climate Change (IPCC). *Climate Change 2021 – The Physical Science*
704 *Basis: Working Group I Contribution to the Sixth Assessment Report of the Intergovernmental Panel on*
705 *Climate Change*. (Cambridge University Press, Cambridge, 2023). doi:10.1017/9781009157896.
706 51. Lenth, R. Least-Squares Means: The R Package lsmeans. *Journal of Statistical Software* **69**, 1–33
707 (2016).
708 52. Lawrence, M. A. ez: Easy Analysis and Visualization of Factorial Experiments. (2016).
709 53. Warton, D. I., Wright, S. T. & Wang, Y. Distance-based multivariate analyses confound location and
710 dispersion effects. *Methods in Ecology and Evolution* **3**, 89–101 (2012).
711 54. Wang, Y., Naumann, U., Wright, S. T. & Warton, D. I. mvabund– an R package for model-based
712 analysis of multivariate abundance data. *Methods in Ecology and Evolution* **3**, 471–474 (2012).
713 55. Rillig, M. C. *et al.* Interchange of entire communities: microbial community coalescence. *Trends in*
714 *Ecology & Evolution* **30**, 470–476 (2015).
715 56. Rillig, M. C. *et al.* Soil microbes and community coalescence. *Pedobiologia* **59**, 37–40 (2016).
716 57. Pold, G., Saghaï, A., Jones, C. M. & Hallin, S. Denitrification is a community trait with partial pathways
717 dominating across microbial genomes and biomes. *Nat Commun* **16**, 9495 (2025).

58. Doherty, S. J. *et al.* The Transition From Stochastic to Deterministic Bacterial Community Assembly During Permafrost Thaw Succession. *Front. Microbiol.* **11**, (2020).
59. Shchepin, O. *et al.* Genetic structure of the protist Physarum albescens (Amoebozoa) revealed by multiple markers and genotyping by sequencing. *Molecular Ecology* **31**, 372–390 (2022).
60. Pearce, D. A. *et al.* Aerobiology Over Antarctica – A New Initiative for Atmospheric Ecology. *Front Microbiol* **7**, 16 (2016).
61. Monteux, S., Mariën, J. & Krab, E. J. Dispersal of bacteria and stimulation of permafrost decomposition by Collembola. *Biogeosciences* **19**, 4089–4105 (2022).
62. Rumpf, S. B., Alsos, I. G. & Ware, C. Prevention of microbial species introductions to the Arctic: The efficacy of footwear disinfection measures on cruise ships. *NeoBiota* **37**, 37–49 (2018).
63. Wegner, R., Fiencke, C., Knoblauch, C., Sauerland, L. & Beer, C. Rapid Permafrost Thaw Removes Nitrogen Limitation and Rises the Potential for N2O Emissions. *Nitrogen* **3**, 608–627 (2022).
64. Rasmussen, L. H., Mortensen, L. H., Ambus, P., Michelsen, A. & Elberling, B. Normalizing time in terms of space: What drives the fate of spring thaw-released nitrogen in a sloping Arctic landscape? *Soil Biology and Biochemistry* **175**, 108840 (2022).
65. Sanders, T. *et al.* Seasonal nitrogen fluxes of the Lena River Delta. *Ambio* **51**, 423–438 (2022).
66. Voigt, C. *et al.* Increased nitrous oxide emissions from Arctic peatlands after permafrost thaw. *PNAS* **114**, 6238–6243 (2017).
67. Palmer, K., Biasi, C. & Horn, M. A. Contrasting denitrifier communities relate to contrasting N2O emission patterns from acidic peat soils in arctic tundra. *ISME J* **6**, 1058–1077 (2012).
68. Elberling, B., Christiansen, H. H. & Hansen, B. U. High nitrous oxide production from thawing permafrost. *Nature Geoscience* **3**, 332–335 (2010).
69. Rodionow, A., Flessa, H., Kazansky, O. & Guggenberger, G. Organic matter composition and potential trace gas production of permafrost soils in the forest tundra in northern Siberia. *Geoderma* **135**, 49–62 (2006).
70. Hallin, S., Philippot, L., Löffler, F. E., Sanford, R. A. & Jones, C. M. Genomics and Ecology of Novel N2O-Reducing Microorganisms. *Trends in Microbiology* **26**, 43–55 (2018).
71. Prosser, J. I., Hink, L., Gubry-Rangin, C. & Nicol, G. W. Nitrous oxide production by ammonia oxidizers: Physiological diversity, niche differentiation and potential mitigation strategies. *Global Change Biology* **26**, 103–118 (2020).

72. Kits, K. D. *et al.* Kinetic analysis of a complete nitrifier reveals an oligotrophic lifestyle. *Nature* **549**, 269–272 (2017).
73. Patchett, A. *et al.* The role of mycorrhizal type and plant dominance in regulating nitrogen cycling in Oroarctic soils. *Biogeosciences* **22**, 6841–6860 (2025).
74. Daims, H. *et al.* Complete nitrification by Nitrospira bacteria. *Nature* **528**, 504–509 (2015).
75. Klaminder, J., Yoo, K., Rydberg, J. & Giesler, R. An explorative study of mercury export from a thawing palsa mire. *Journal of Geophysical Research: Biogeosciences* **113**, G04034 (2008).
76. Olid, C., Klaminder, J., Monteux, S., Johansson, M. & Dorrepaal, E. Decade of experimental permafrost thaw reduces turnover of young carbon and increases losses of old carbon, without affecting the net carbon balance. *Global Change Biology* **26**, 5886–5898 (2020).
77. Mondav, R. *et al.* Discovery of a novel methanogen prevalent in thawing permafrost. *Nat Commun* **5**, 3212 (2014).

Acknowledgements

Sequencing was performed by the SNP&SEQ Technology Platform in Uppsala. The facility is part of the National Genomics Infrastructure (NGI) Sweden and Science for Life Laboratory. The SNP&SEQ Platform is also supported by the Swedish Research Council and the Knut and Alice Wallenberg Foundation.

The data handling was enabled by resources provided by the Swedish National Infrastructure for Computing (SNIC) at UPPMAX partially funded by the Swedish Research Council through grant agreement no. 2018-05973

We thank Anders Möberg, Mohammad Rezwan and the Bolin Centre for Climate Research Code Database for hosting the reproducible code and data repository.

We thank Thomas Douglas for access to the CRREL facility, Magnus Widesheim for his work on the anoxic incubation, the Swedish Polar Research Secretariat and SITES for the logistical support of the work done at the Abisko Scientific Research Station, and the Toolik Field Station for support in field work.

The work was supported by funding from Formas (Dnr 2017–01182) awarded to EJK, the Swedish Research Council (VR 2022-03940) and European Research Council (ERC StG PRIMETIME

101039588) awarded to BW, and the Swedish Research Council (VR 621–2011–5444) and Formas (Dnr 214–2011–788) awarded to ED.

Author contributions

SM: conceptualization, data curation, formal analysis, investigation, methodology, project administration, software, visualization, validation, writing - original draft, writing - review and editing.
ED: conceptualization, funding acquisition, writing - original draft, writing - review and editing.
SF: investigation, data curation, writing - review and editing.
KG: formal analysis, data curation, writing - original draft and writing - review and editing.
SH: funding acquisition, methodology, writing - review and editing.
JJ: investigation, methodology, formal analysis, data curation, writing - review and editing.
FK: conceptualization, methodology, writing - original draft, writing - review and editing.
JW: investigation, data curation, writing - review and editing.
RW: investigation, visualization, writing - review and editing.
BW: funding acquisition, investigation, writing - review and editing.
EK: conceptualization, funding acquisition, project administration, writing - original draft, writing - review and editing.

Competing interests

We declare no competing interests.

Materials & correspondence

Correspondence and material requests should be addressed to Sylvain Monteux sylvain.monteux@uit.no

Supplementary material

Active layer microbial inocula restore missing functions across thawed permafrost soils

Sylvain Monteux[1,2,3,4], Ellen Dorrepaal[5], Sébastien Fontaine[6], Konstantin Gavazov[7], Sara Hallin[8], Jaanis Juhanson[8], Frida Keuper[9], Josefine Walz[5], Rica Wegner[2], Birgit Wild[2,3], Eveline J. Krab[1]

1: Department of Soil and Environment, Swedish University for Agricultural Sciences, Uppsala, Sweden
2: Department of Environmental Science, Stockholm University, Stockholm, Sweden
3: Bolin Centre for Climate Research, Stockholm University, Stockholm, Sweden
4: Tromsø Museum, UiT The Arctic University of Norway, Tromsø, Norway
5: Climate Impacts Research Centre, Umeå University, Abisko, Sweden
6: Grassland Ecosystem Research Unit, French National Institute for Food, Agriculture and Environment INRAE, Clermont-Ferrand, France
7: Swiss Federal Institute for Forest, Snow and Landscape Research WSL, Birmensdorf, Switzerland
8: Department of Forest Mycology and Plant Pathology, Swedish University for Agricultural Sciences, Uppsala, Sweden
9: BioEcoAgro Joint Cross-Border Research Unit, French National Institute for Food, Agriculture and Environment INRAE, Laon, France

Table of contents

Supplementary Text

Complementary oxic incubation: inoculum artefacts

Methods

The introduction of labile substrates, such as those derived from dead microbial cells, might be increased by the addition of 1 ml soil suspensions used as inoculum in active layer and positive control treatments. We tested this using the Yedoma sediment where functional limitations were known, by incubating two sets of jars mimicking the negative and positive controls used above ('Control' and 'Live', respectively), and one set where the inoculum consisted in the same soil used for positive controls but that had undergone gamma-irradiation at 45 kGy ('Sterile'). The jars were incubated for 389 days at 10 °C under dark oxic conditions in 4 replicates, and CO_2 production was monitored as described for the main experiment. The entire design was duplicated, using in one case liquid inoculum as in the rest of the manuscript, and in the second case a solid soil transfer as in ref. [10].

The CO_2 flux data was analysed with RM-ANOVA for solid inoculum, and no interaction between inoculation treatment and time was detected ($P = 0.225$). The loss of one jar during the incubation unbalanced the design for liquid inoculum, thus we used a two-way ANOVA on cumulative emissions at day 356, using inoculum type (liquid or solid) and inoculum treatment (control, sterile or positive control) as fixed factors, followed by appropriate pairwise contrasts with *emmeans*.

Results

The inoculation method (i.e. liquid or solid) significantly interacted with the type of inoculum (control, gamma-irradiated or live positive control soil, Supplementary Figure S6). CO_2 production in the live positive control was significantly higher than in both the control and gamma-irradiated soil inoculum, but this increase was less

pronounced when using a solid inoculum (+31% ± 2% compared to negative control, estimated marginal mean ± SE, n = 4) than a liquid inoculum (+61% ± 3%). The CO_2 production in soils inoculated with gamma-irradiated inoculum in either liquid or solid form did not differ from the negative control ($P \geq 0.735$).

Anoxic incubation: control on inoculum artefacts

To circumvent putative biases caused by introduced substrates upon inoculation, the experimental design of the anoxic incubation accounted for such biases. Instead of using ultrapure water as a negative control and a filtered solution of active layer soil suspension for inoculation, we used an active layer soil suspension in both cases. Soil from the active layer was separated into two flasks, once of which was shipped to Scandinavian Clinics Estonia for sterilization by gamma-irradiation at 45 kGy. While gamma-irradiation inevitably leads to modifications in soil chemistry, it is the least damaging solution for sterilization.

Permafrost soil was thawed at room temperature in an N_2-atmosphere. The excess water after thawing was decanted and filtered (8 µm Whatman grade 40 paper filter) into an autoclaved glass bottle: this constitutes suspension (1). *Soil slurries were created from both the sterilized ('Control') and the live active layer soil ('Palsa'), by putting 1 g of soil into 70 ml of suspension (1), shaking (150 rpm orbital shaker 90 min) and soaking for at least 2 hours at room temperature, before filtering (8 µm Whatman grade 40)*. Control and Palsa suspensions were stored at 4 °C overnight, before adding 2 ml of those to half of the 16 jars containing 15 g of homogenized permafrost, selected at random. All steps were performed using autoclaved material, steps in italic font were not performed under a N_2-atmosphere but using sterile technique.

Supplementary Tables

Supplementary Table S1: Abiotics variables in pre-incubation permafrost and active layer inoculum. Numbers indicate mean ± SE, n=4. GWC: Gravimetric water content; OMC: organic matter content; DOC: Dissolved organic carbon; TN: total dissolved nitrogen. †: n=3; ‡: n=1.

		GWC [%]	OMC [%]	DOC [mg.kgDW^{-1}]	TN [mg.kgDW^{-1}]	NH_4 [mg.kgDW^{-1}]	NO_3 [mg.kgDW^{-1}]	pH	Bulk density [g.cm^{-3}]
Permafrost	Cryoturbated	19.5 ± 1.37	1.39 ± 0.03 †	129.18 ± 3.65	14.8 ± 0.57	2.18 ± 0.31	0.28 ± 0.06	8.01 ± 0.03	1.43
	Tussock	40.17 ± 0.57	15.16 ± 0.07	470.4 ± 12.56	60.4 ± 1.69	20.08 ± 0.8	0.45 ± 0.06	7.19 ± 0.05	n.d.
	Palsa	28.42 ± 0.42	3.91 ± 0.06	320.95 ± 12.05	35.43 ± 0.98	14.25 ± 0.33	0.58 ± 0.05	6.45 ± 0.06	0.14
	Yedoma	39.59 ± 1.51	7.85 ± 0.05	1286.25 ± 24.65	151.35 ± 2.69	79.58 ± 2.31	0.28 ± 0.05	6.83 ± 0.02	0.78
Active layer / Inoculum	Cryoturbated †	23.46 ± 1.19	6.82 ± 0.62	25.45 ± 5.05	2.2 ± 1.1	< d.l. ‡	1.50 ‡	7.67 ‡	n.d.
	Tussock †	81.32 ± 2.00	86.81 ± 1.86	7688.35 ± 110.85	9.3 ± 6.4	< d.l. ‡	< d.l. ‡	5.46 ‡	n.d.
	Palsa †	79.1 ± 0.84	95.91 ± 0.11	452.85 ± 56.05	5.6 ± 6.5	< d.l. ‡	< d.l. ‡	4.91 ‡	n.d.
	Positive control †	25.81 ± 0.19	13.5 ± 0.20	15.15 ± 5.25	11.05 ± 3.25	1.10 ‡	5.10 ‡	6.12 ‡	n.d.

Supplementary Table S2: Primers and conditions for the PCR reactions for 16S amplicon and for the qPCR assays for inhibition test, 16S rRNA gene, *amoA*, *nir* and *nos* functional genes. The qPCR reactions were carried out in two technical replicates with an initial denaturation at 95 °C for 5 min, and cycles of denaturation at 95 °C for 15 s, annealing for 30 s and elongation at 72 °C, fluorescence signal was read for 5 s at the end of each non-touchdown cycle, at 77 °C for amoA and nosZ-II and at 80 °C for nirS, nirK and nosZ-I. Standard curves R^2 and efficiency were derived by serial dilutions of linearized plasmids containing cloned fragments of the specific genes in the range of 10^1-10^7 copies per reaction.

		16S rRNA gene V4V5 amplicons	Indexing PCR
Primers and sequences 5' - 3'		515F GTGYCAGCMGCCGCGGTAA 926R CCGYCAATTYMTTTRAGTTT	N501-N504, N506, N507, N510, N511 N701-N712
Reference		Parada et al., 2016, Quince et al., 2011	Nextera XT Index Kit v2, Illumina
Phusion Green PCR Master Mix		12.5 µl	15 µl
Nuclease-free water		9.25 µl	7 µl
DNA template volume		2 µl	5 µl
DNA template dilution		5 ng . µl^{-1} *	-
Primer concentration		10 µM	3 µM
Primer volume		0.625 µl	3 µl
Reaction volume		25 µl	30 µl
Initial denaturation		98 °C 3 min	98 °C 3 min
Cycles	Denaturation	98 °C 15 s	98 °C 30 s
	Annealing	×25† 50 °C 30 s	×8 55 °C 30 s
	Elongation	72 °C 40 s	72 °C 30 s
Final elongation		72 °C 10 min	72 °C 10 min
PCR clean-up		SequalPrep Normalization Plate Kit 20 µl elution	SequalPrep Normalization Plate Kit 20 µl serial elution across columns
PCR product quantification		NA	Qubit dsDNA HS Agilent 2100 Bioanalyzer

*: undiluted and- †: 30 cycles- for most Cryoturbated samples

qPCR assay target	Target gene	Primer	Primer sequence 5' - 3'	Primer reference	Final primer conc.	Cycles	Annealing temp.	Elongation time	R^2 / Efficiency %
Inhibition	TOPO vector	M13F M13R	GTAAAACGACGGCCAG CAGGAAACAGCTATGAC		0.1 µM	35	55 °C	45 s	NA
Prokaryotes	16S rRNA V4V5	515F 926R	GTGYCAGCMGCCGCGGTAA CCGYCAATTYMTTTRAGTTT	Parada *et al.*, 2016 Quince *et al*., 2011	0.2 µM	35	55 °C	30 s	0,995 / 94,4
Ammonia-oxidizing bacteria (AOB) *	*amoA*	amoA-1F amoA-2R	GGGGTTTCTACTGGTGGT CCCCTCKGSAAAGCCTTCTTC	Rotthauwe *et al*., 1997	0.5 µM	40	55 °C	40 s	0,995 / 108.0
Ammonia-oxidizing archaea (AOA)	*amoA*	CrenamoA23f CrenamoA616R	ATGGTCTGGCTWAGACG GCCATCCATCTGTATGTCCA	Tourna *et al*., 2008	0.5 µM	40	55 °C	40 s	0,993 / 88,7
Nitrite reductase S ‡	*nirS*	cd3aFm R3cdm	AACGYSAAGGARACSGG GASTTCGGRTGSGTCTTSAYGAA	Throbäck et al., 2004	0.5 µM	6 c. → 35	65-1°C / c. → 60 °C	30 s	0.997 / 83,6
Nitrite reductase K †	*nirK*	F1aCu 1040R	ATCATGGTSCTGCCGCG GCCTCGATCAGRTTRTGGTT	Henry et al., 2006	0.5 µM	6 c. → 35	63-1°C / c. → 58 °C	35 s	0.997 / 83,3
Nitrous oxide reducers clade I ‡	*nosZ*	1840F 2090R	CGCRACGGCAASAAGGTSMSSGT CAKRTGCAKSGCRTGGCAGAA	Henry et al., 2006	0.5 µM	6 c. → 35	65-1°C / c. → 60 °C	30 s	0.997 / 78,6
Nitrous oxide reducers clader II †	*nosZ*	nosZ-II_F nosZ-II_R	CTIGGICCIYTKCAYAC GCIGARCARAAITCBGTRC	Jones et al., 2013	2 µM	40	54 °C	45 s	0.998 / 82,1

*specific-size bands could not be obtained for most samples. R^2/efficiency based on one replicate

Supplementary Table S3: Quantitative data obtained from qPCR analyses. Empty cells indicate that no quantitative data could be obtained, italicized values were below the detection limit of 10 copies per reaction. DNA: DNA concentration in extracts; 16S: 16S rRNA gene V4V5 region; AOA: ammonia-oxidizing archaea *amoA* gene; nirS: nitrite reductase S gene; nirK: nitrite reductase K gene; nosZ-I: nitrous oxide reductase clade I gene; nosZ-II: nitrous oxide reductase clade II gene.

Soil	Date	Treatment	Replicate	DNA [ng.ul^{-1}]	Gene copy number per reaction					
					16S	AOA	*nirS*	*nirK*	*nosZ*-I	*nosZ*-II
Cryoturbated	Pre-incubation permafrost		1	0.059	23					
			2	0.054	29					
Tussock	Pre-incubation permafrost		1	1.61	65995				27	
			2	2.16	175951		*2*	84	23	14
			3	1.31	68453					12
Palsa	Pre-incubation permafrost		2	0.108	501					
Yedoma	Pre-incubation permafrost		1	0.263	985					
			2	0.722	13790					
			3	0.666	1921					
Cryoturbated active layer inoculum			1	46.9	201643	789	207	1889	235	1057
			2	56	155588	560	205	1556		736
			3	34.7	135314	309	224	1374	19	633
			4	15.8	247793	1557	304	2273	422	1638
Tussock active layer inoculum			1	47.9	116127				52	
			2	33.2	105807			337	42	
			3	40.1	93251				17	
			4	39.3	95130				27	
Palsa active layer inoculum			1	> 60	71953			160		
			2	56	71714		*6*	158		
			3	57	141290			276		
			4	55	99661		13		*7*	
Positive control inoculum			1	> 60	139888	2265	41	2178		721
			3	> 60	95130	1729	32	1438		492
			4	> 60	94499	1393	27	1149		425
Cryoturbated	Day 1	Control	1	0.097	40					
			2	0.061	270					
			3	0.051	42					
		Cryoturbated	2	0.077	46					
			4	4.66	210547	26	30	1855	244	657
	Day 389	Control	1	0.062	27					
			2	0.054	49			*2*		
			3	0.108	45					
			4	0.128	22					
		Positive control	1	0.116	53					
Tussock	Day 1	Control	1	3.05	452263			156	20	
			2	2.41	472236			*8*	73	
			3	4.11	208458			158	19	
			4	4.83	199642			84	25	
		Tussock	1	4.3	293573			106	17	58
			3	3.14	253627		11	116	34	
			4	4.46	261329			91	18	
		Positive control	1	3.49	323282	436	12	211	62	40
			2	6.26	295531	321		154	25	
			3	3.76	357184	368	*10*	218	66	27
			4	3.02	287775	152		127	28	
	Day 389	Control	1	22	184947		18	268	788	240
			2	20.4	288734		29	539	1142	206
			3	19.6	205022		42	539	1297	223
			4	16.6	208458		24	727	795	227
		Tussock	2	28.1	278367		56	453	1206	263
			3	21.6	155588		13	231	697	154
			4	17.9	211952		50	230	804	284
		Positive control	2	26.7	178306	78	67	1720	534	1251
			3	15	302488	31	244	2785	681	626
			4	17.9	209152	56	139	2192	226	1360

Supplementary Table S3 (continued): Quantitative data obtained from qPCR analyses.

Soil	Date	Treatment	Replicate	DNA [ng.ul^{-1}]	Gene copy number per reaction					
					16S	AOA	*nirS*	*nirK*	*nosZ*-I	*nosZ*-II
Palsa	Day 1	Control	1	0.125	4791					
			2	0.151	577					
			3	0.117	2384					*2*
			4	0.137	311					
		Palsa	1	0.169	2143					*3*
			2	0.198	3090					
			3	0.182	3747					
			4	0.173	556					
		Positive control	1	0.463	29818	227		76	21	33
			2	0.265	10570	52	*1*	32	*10*	*8*
			3	0.163	12113	96	*2*	51	*9*	14
			4	0.142	5677	41		13		*5*
	Day 389	Control	1	6.28	150002		11	550	280	
			2	1.63	211248			2266	401	
			3	4.31	122065			982	190	670
			4	6.02	164087		14	988	240	1277
		Palsa	1	7.46	107938			616	275	949
			2	4.87	113456		14	682	194	478
			3	6.49	151505			1129	540	2076
			4	6.97	143658			633	354	666
		Positive control	1	3.61	134418	53		2172	373	231
			2	2.65	149504	100		1501	364	246
			3	3.98	171334	97		2126	248	241
			4	6.48	175367	144		1699	232	403
Yedoma	Day 1	Control	1	1.07	222049			*4*		
			2	1.27	130023					
			3	1.68	407979				*10*	
			4	1.5	440395					
		Cryoturbated	1	0.764	63204	22		18		
			2	1.82	388135	36		32	24	*9*
			3	0.853	114594			*6*		
			4	0.704	127455	39	*1*	32	26	*9*
		Tussock	1	1.33	319012					
			2	1.76	762159			12	11	
			3	1.3	152010					
			4	1.91	438933					
		Palsa	1	2.45	334209			20	*7*	
			2	1.45	220577					11
			3	1.23	228033		*1*	*5*		
			4	1.08	366810					
		Positive control	1	1.88	333100	233		26	14	
			2	1.17	151002	567		52	16	22
			3	1.22	106867	379		47	14	19
			4	13.1	105807	106		11	*4*	*8*
Yedoma	Day 389	Control	1	29.9	380471			54	296	
			2	12.2	364379			166	28	391
			3	38.1	380471			796	344	
			4	38.8	388135		16	85		
		Cryoturbated	1	21.1	196351		77	1941	126	321
			2	19.7	395954		132	2645	280	740
			3	21.6	186181		49	1628	92	734
			4	22.5	239691		149	2959	272	1214
		Tussock	1	22.1	455280			239	*7*	536
			2	16.8	443332		16	164	14	196
			3	16.7	472236		*5*	183	70	118
			4	6.92	416198			3013	262	164
		Palsa	1	5.04	493090		*10*	544	230	56
			2	16.7	458317			56	423	67
			3	28.4	456796			2400	818	
			4	14.8	478557			68	408	655
		Positive control	1	4.54	200973		37	2393	376	540
			2	8.36	186181		263	1901	217	710
			3	8.85	271964	86	316	3782	420	1825
			4	4.94	295531	24	25	2343	336	949

Supplementary Table S4: Analyses of variance (ANOVA) of biogeochemical variables in four permafrost soils subjected to microbial community manipulation. Values in bold indicate significant ($P < 0.05$) tests, n=4, except for Ammonium-Yedoma-Day389 where n=3. †: Kruskal-Wallis X^2.

		Day 1			Day 389		
		F	df	P	F	df	P
Cumulative CO_2 production	*Cryoturbated*	N.A.			11.647	2	**0.003**
	Tussock				23.59	2	**<0.001**
	Palsa				36.844	2	**<0.001**
	Yedoma				92.945	4	**<0.001**
Gravimetric water content	*Cryoturbated*	2.246	2	0.162	1.759	2	0.227
	Tussock	0.335†	2	0.846	1.841	2	0.214
	Palsa	3.204†	2	0.202	0.281	2	0.761
	Yedoma	0.341	4	0.846	0.259	4	0.900
Organic matter content	*Cryoturbated*	N.A.			1.197	2	0.346
	Tussock				0.597	2	0.571
	Palsa				0.294	2	0.752
	Yedoma				0.224	4	0.921
Dissolved organic carbon	*Cryoturbated*	0.658	2	0.541	0.389	2	0.689
	Tussock	8.031	2	**0.010**	1.784	2	0.223
	Palsa	11.773	2	**0.003**	0.565	2	0.587
	Yedoma	3.772	4	**0.026**	6.236	4	**0.004**
Total dissolved nitrogen	*Cryoturbated*	1.7	2	0.236	0.39	2	0.688
	Tussock	2.387	2	0.147	3.471	2	0.076
	Palsa	12.926	2	**0.002**	0.864	2	0.454
	Yedoma	2.727	4	0.069	2.992†	4	0.559
Ammonium	*Cryoturbated*	0.1085	2	0.898	N.A.		
	Tussock	0.802	2	0.478	3.052	2	0.097
	Palsa	11.214	2	**0.004**	1.334	2	0.311
	Yedoma	1.054	4	0.413	0.65	4	0.636
Dissolved inorganic nitrogen	*Cryoturbated*	0.207	2	0.817	7.2†	2	**0.027**
	Tussock	2.102†	2	0.35	6.362†	2	**0.042**
	Palsa	10.883	2	**0.004**	1.334	2	0.311
	Yedoma	1.123	4	0.383	2.514†	4	0.642
pH	*Cryoturbated*	0.447	2	0.653	3.343	2	0.082
	Tussock	2.285	2	0.158	0.664	2	0.538
	Palsa	8.054	2	**0.010**	2.262	2	0.16
	Yedoma	4.807†	4	0.308	6.739†	4	0.15
Organic nitrogen	*Cryoturbated*	1.011	2	0.374	0.038†	2	0.981
	Tussock	5.669	2	**0.026**	1.907	2	0.204
	Palsa	3.485	2	0.076	0.78	2	0.487
	Yedoma	4.252	4	**0.017**	1.418	4	0.276

Supplementary Table S5: Effects of microbial community manipulation on bacterial community composition, alpha-diversity and 16S rRNA gene abundance in four permafrost soils. Values in bold indicate significant (P<0.05) tests, n=4. †: Kruskal-Wallis X^2.

		Day 1			Day 389		
	Soil type	**Dev**	**df**	***P***	**Dev**	**df**	***P***
Bacterial community (ManyGLM)	*Cryoturbated*	3900	2	0,131	1936	2	0,064
	Tussock	15779	2	**0,005**	29951	2	**0,002**
	Palsa	24140	2	**0,002**	23226	2	**0,004**
	Yedoma	15785	4	**0,003**	36970	4	**0,001**
		F	**df**	***P***	**F**	**df**	***P***
Alpha-diversity Coverage Estimator ACE	*Cryoturbated*	3.727†	2	0,155	0,4003	2	0,683
	Tussock	70,982	2	**<0.001**	63,855	2	**<0.001**
	Palsa	21,787	2	**<0.001**	44,464	2	**<0.001**
	Yedoma	5,025	4	**0,009**	89,624	4	**<0.001**
16S rRNA gene copy number	*Cryoturbated*		N.A.			N.A.	
	Tussock	0,078	2	0,926	0,439	2	0,661
	Palsa	5,854	2	**0,024**	2,4215	2	0,144
	Yedoma	1,083	4	0,400	15,68	4	**<0.001**

Supplementary Table S6: Examples of published values of N_2O fluxes in permafrost systems.

Gross N_2O fluxes are measured in presence of acetylene to inhibit N_2O-reductase. Values from the experiments with settings most directly comparable to that found in this study (i.e. aerobic incubation without vegetation) are italicized. WFPS: Water-filled pore space; WC: water content; *: whole core in mesocosm; **: mg-N_2O-N.m^{-2}.d^{-1}; b.d.l.: below detection limit; -: not measured.

Lead author	doi	Permafrost soil type	Location	Depth	Vegetation	Incubation conditions			WFPS	WC	Net N_2O flux		Gross N_2O flux	
				[cm]		Temp.	Length	Atmosphere			[µg N_2O-N . kg DW^{-1} . d^{-1}]			
						°C	d		%	%	Min	Max	Min	Max
Wegner	10.3390/nitrogen3040040	Thaw slump, eroded Yedoma + Holocene, mineral soil	Siberia	0-30	Yes	4	40	anaerobic	52-67	21-28	0,00	0,00	-	-
Wegner	10.3390/nitrogen3040040	Thaw slump, eroded Yedoma + Holocene, mineral soil	Siberia	0-30	No	4	40	anaerobic	52-67	21-28	0,10	95,43		
Wegner	10.3390/nitrogen3040040	Thaw slump, Yedoma, Mineral soil	Siberia	0-30	Yes	4	40	anaerobic	45-74	17-29	27,85	216,63	-	-
Wegner	10.3390/nitrogen3040040	Thaw slump, Yedoma, Mineral soil	Siberia	0-30	No	4	40	anaerobic	45-74	17-29	0,00	25,16	-	-
Wegner	10.3390/nitrogen3040040	Thaw slump, Yedoma, Mineral soil	Siberia	20-40	No	4	40	anaerobic	n.d.	17	-	63,66	-	-
Wegner	10.3390/nitrogen3040040	Thaw slump, Yedoma, Mineral soil	Siberia	40-70	No	4	40	anaerobic	43	16	-	22,17	-	-
Rasmussen	10.1016/j.soilbio.2022.108840	Glacial Valley, mineral soil	Greenland	0-15		5	31	aerobic	-	-	*480,00*	*9600,00*		
Sanders	10.1007/s13280-021-01665-0	Floodplain, mineral soil	Siberia	25-30	No	5	126	aerobic	-	-	*0,00*	*0,04*	-	-
Marushchak	10.1038/s41467-021-27386-2	Thaw slump, eroded Yedoma + Holocene, mineral soil	Siberia	0-10	Yes	10	1-6	aerobic	52-94	-	0,12	0,14	-	-
Marushchak	10.1038/s41467-021-27386-2	Thaw slump, eroded Yedoma + Holocene, mineral soil	Siberia	0-10	No	10	1-6	aerobic	52-94	-	*-0,19*	*0,02*	-	-
Marushchak	10.1038/s41467-021-27386-2	Thaw slump, Holocene, mineral soil	Siberia	0-10	Yes	10	1-6	aerobic	13	-	-	0,12	-	-
Marushchak	10.1038/s41467-021-27386-2	Thaw slump, eroded Yedoma + Holocene, mineral soil	Siberia	0-10	Yes	10	1-6	anaerobic	52-94	-	95,28	606,48	393,60	2820,96
Marushchak	10.1038/s41467-021-27386-2	Thaw slump, eroded Yedoma + Holocene, mineral soil	Siberia	0-10	No	10	1-6	anaerobic	52-94	-	3,12	19,20	6,00	10,08
Marushchak	10.1038/s41467-021-27386-2	Thaw slump, Holocene, mineral soil	Siberia	0-10	Yes	10	1-6	anaerobic	13	-	-	606,48	-	2820,96
Voigt	10.1073/pnas.1702902114	Peat palsa	Finland	0-100*	Mesocosm	10	28	aerobic	-	-	0,14**	0,20**		
Voigt	10.1073/pnas.1702902114	Peat palsa	Finland	0-100*	Mesocosm	10	28	aerobic	-	-	0,56**	2,81**		
Palmer	10.1038/ismej.2011.172	peat plateau, cryoturbated peat soil	Russia	0-5	No	20	3,75	anaerobic	-	-	-	8964,29	-	13446,43
Palmer	10.1038/ismej.2011.172	peat plateau, non-turbated peat soil	Russia	0-5	Yes	20	3,75 - 6,6	anaerobic	-	-	-	0,00	-	58,83
Elberling	10.1038/NGEO803	Wetland, active layer, mineral soil	Greenland	0-60	Yes	7	150	aerobic	-	-	-	32,88 (144)	-	-
Elberling	10.1038/NGEO803	Heath tundra, active layer, mineral soil	Greenland	0-80	Yes	7	150	aerobic	-	-	-	b.d.l.	-	-
Elberling	10.1038/NGEO803	Wetland, permafrost, mineral soil	Greenland	60-300	Yes	7	150	aerobic	-	-	-	20,88	-	-
Elberling	10.1038/NGEO803	Heath tundra, permafrost, mineral soil	Greenland	80-300	Yes	7	150	aerobic	-	-	-	b.d.l.	-	-
Rodionow	10.1016/j.geoderma.2005.10.008	Forest – heath tundra ecotone	Siberia	0-50	No	5-15	0.25-0.4	aerobic	-	60-100	-	*0,72*	-	-
This study		Palsa permafrost, day 7, control	Sweden	110-130	No	10	7	aerobic	-	28-32	0,89	1,56	-	-
This study		Palsa permafrost, day 7, active layer inoculum	Sweden	110-130	No	10	7	aerobic	-	28-30	1,15	8,89	-	-
This study		Palsa permafrost, day 7, positive control	Sweden	110-130	No	10	7	aerobic	-	28-29	4,29	6,76	-	-
This study		Palsa permafrost, day 17, active layer inoculum	Sweden	110-130	No	10	17	aerobic	-	28-30	0,44	0,46	-	-
This study		Palsa permafrost, day 17, positive control	Sweden	110-130	No	10	17	aerobic	-	28-29	9,46	13,86	-	-
This study		Tussock tundra permafrost, day 187, positive control	Alaska	70-100	No	10	187	aerobic	-	36-38	1,09	7,46	-	-

Supplementary Figures

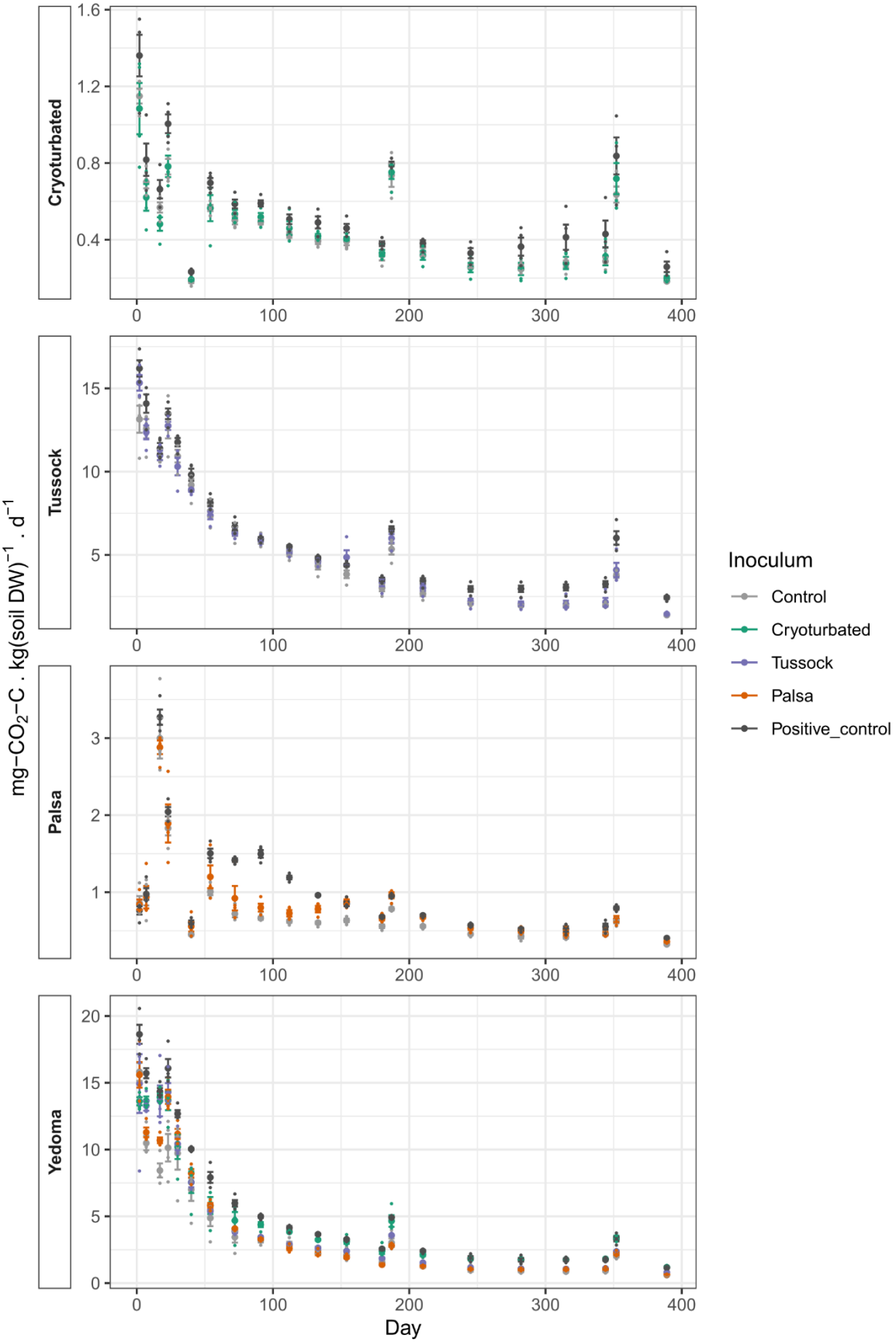

Supplementary Figure S1: Daily CO_2 production of four permafrost soils subjected to microbial community manipulation over 389 days of oxic incubation. Large symbols and error-bars indicate mean +/- SE (n=4), small symbols are individual measurements. Higher values at days 187 and 352 are presumably due to the shorter time interval between measurements, giving a disproportionately high role to the diffusion from pore space to CO_2-free headspace immediately after flushing. Conversely, lower values at day 40 for Turbel and Palsa soils are presumably due to the longer time interval between measurements.

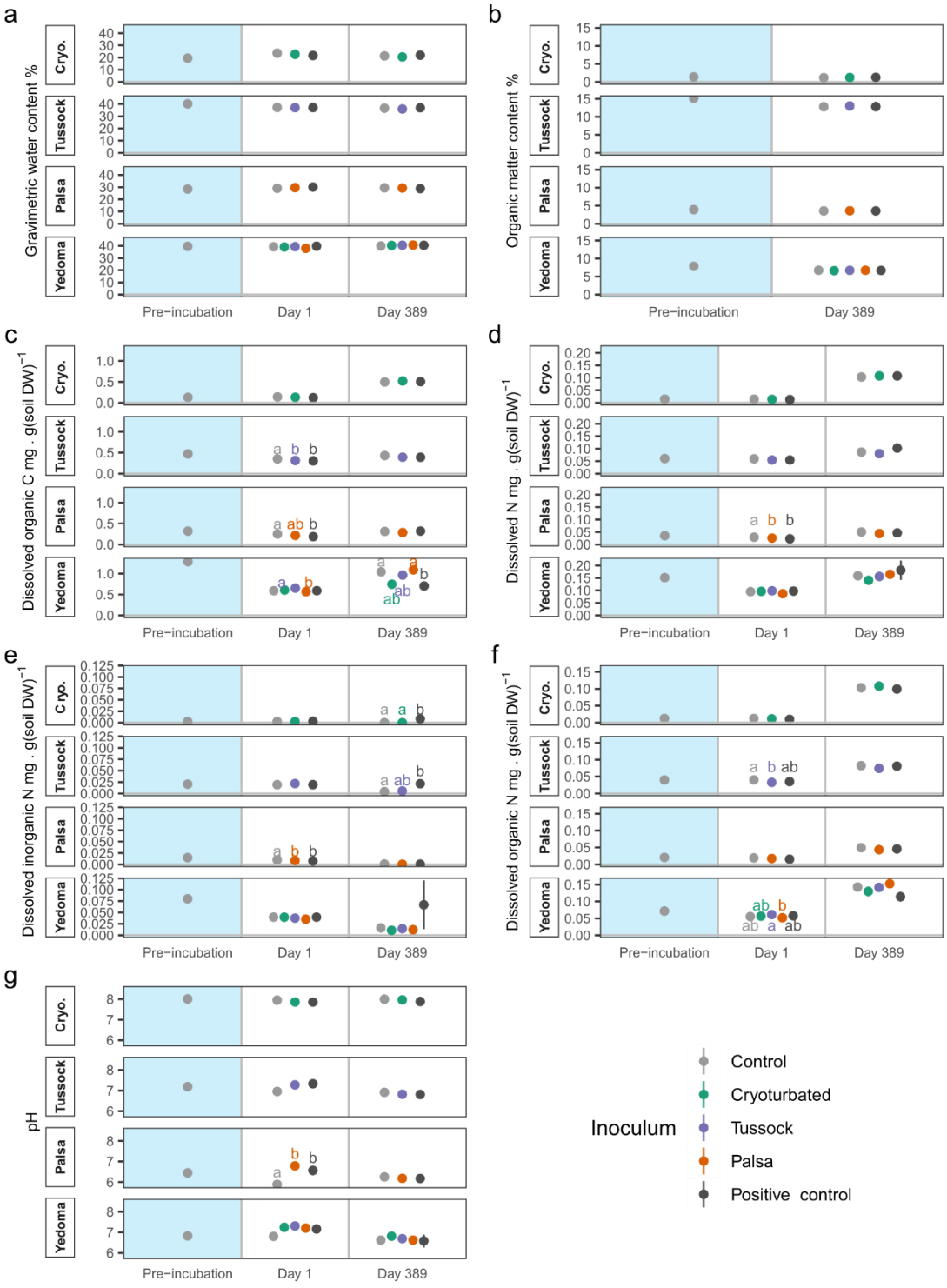

Supplementary Figure S2: Physical and chemical variables of four permafrost soils subjected to microbial community manipulation over 389 days of oxic incubation. (**a**) Gravimetric water content, (**b**) organic matter content, (**c**) water-extractable dissolved organic C, (**d**) water-extractable dissolved nitrogen. (**e**) dissolved inorganic nitrogen content, (**f**) dissolved organic nitrogen content, (**g**) pH. Symbols and error-bars represent mean +/- SE (n=4), different letters denote statistically significant differences within a soil:date group (Holm-adjusted $P < 0.05$). Organic matter content was not measured at day 1 in (**b**), as it was presumedly unchanged from pre-incubation values.

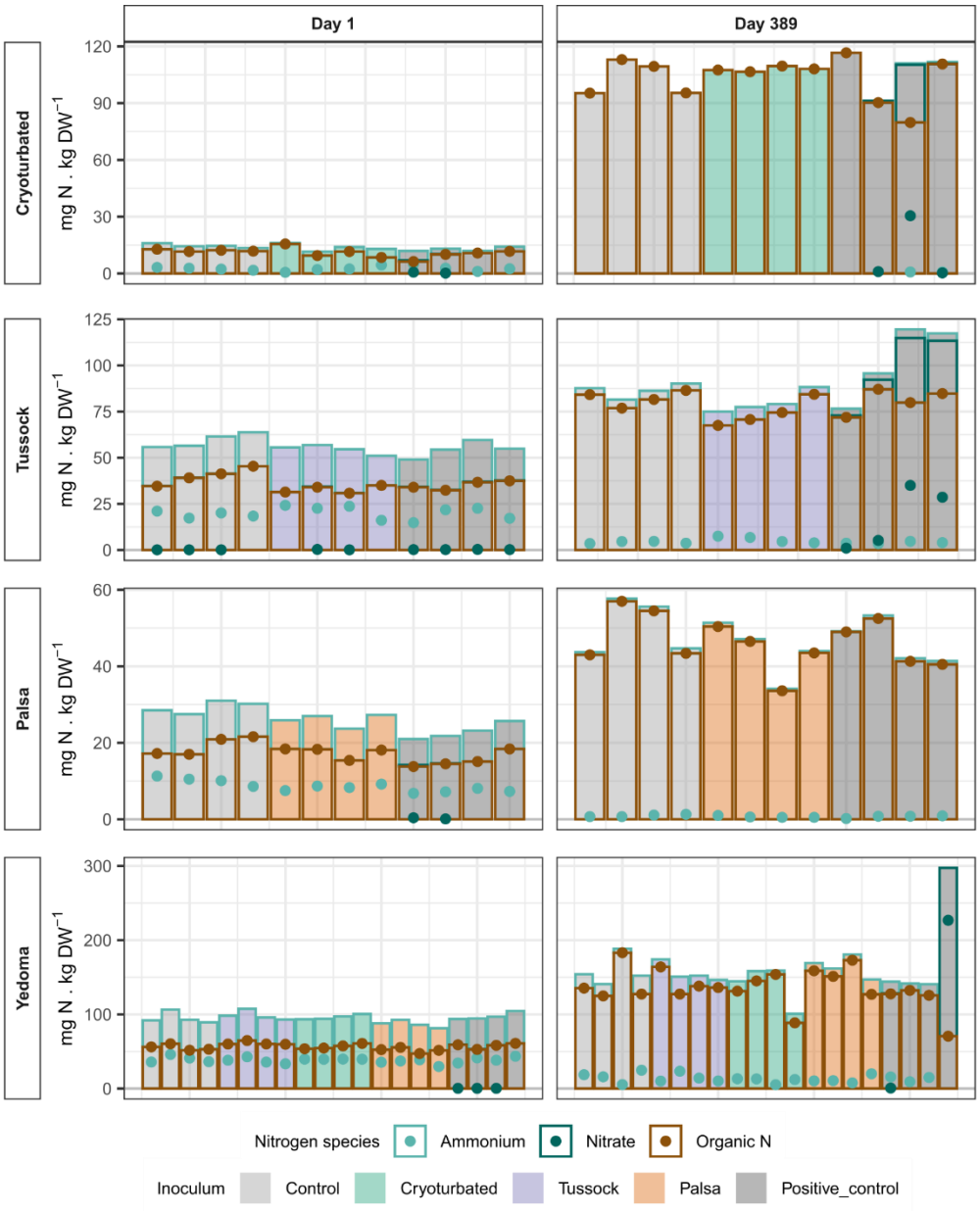

Supplementary Figure S3: Distribution of water-extractable nitrogen species in four permafrost soils subjected to microbial community manipulation over 389 days of oxic incubation. Points represent individual values for each sample, bars depict the same values added to each other for comparison of the relative contributions to the total dissolved N pool. Each set of bars and points represent an invidivual replicate.

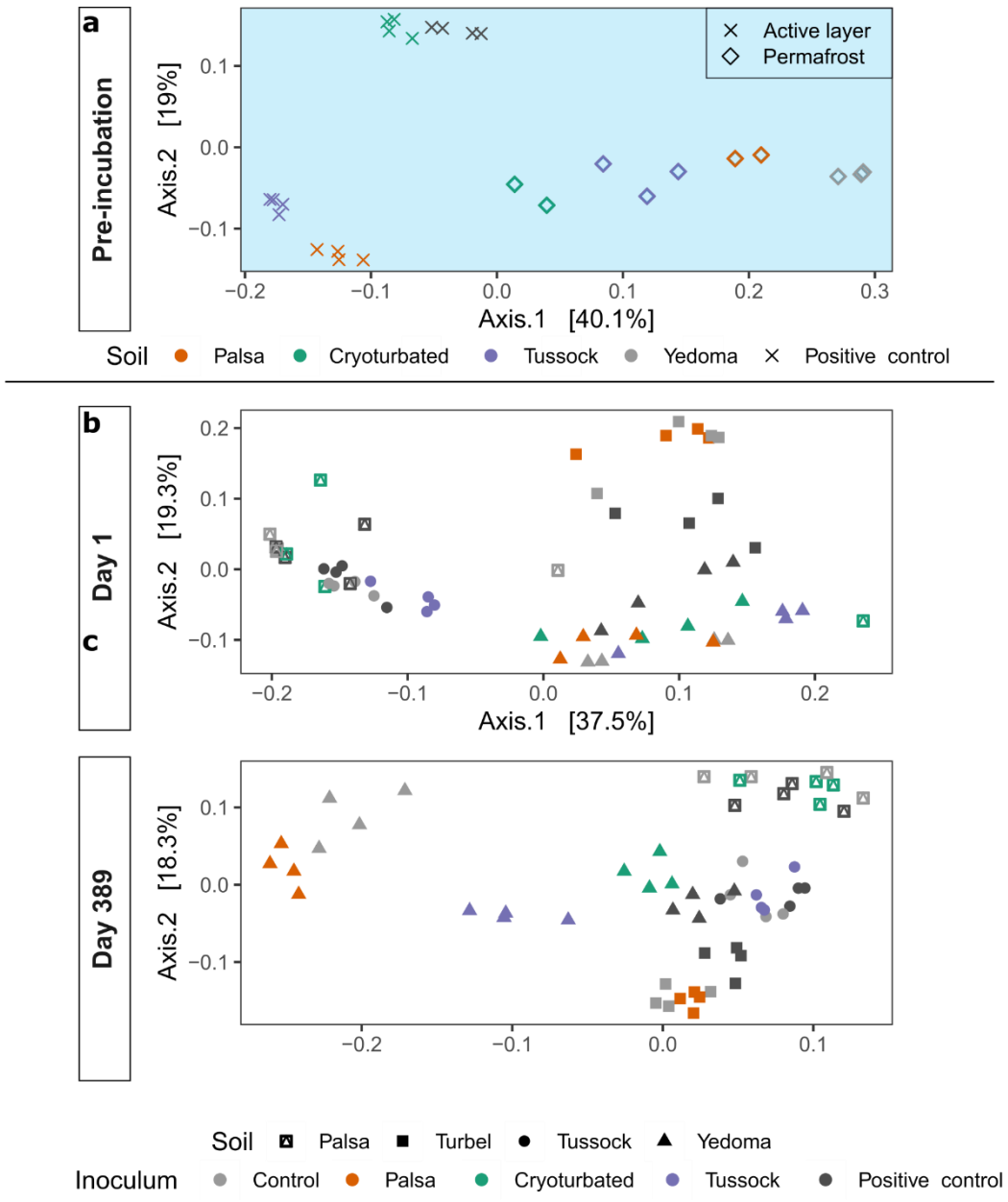

Supplementary Figure S4: Bacterial communities of four permafrost soils subjected to microbial community manipulation before (a), after 1 day (b) and after 389 days (c) of oxic incubation.
Principal coordinate analyses (PCoA) of weighted UniFrac distances of amplicon sequence variants (ASVs) computed from amplicons of 16S rRNA gene V4-V5 region.
(a) Pre-incubation permafrost and active layer samples, permafrost samples were processed in triplicates and samples failed sequencing quality control for Palsa and Cryoturbated resulting in n=2.
(b,c) Incubated jars after one day and 389 days of aerobic incubation, n=4.

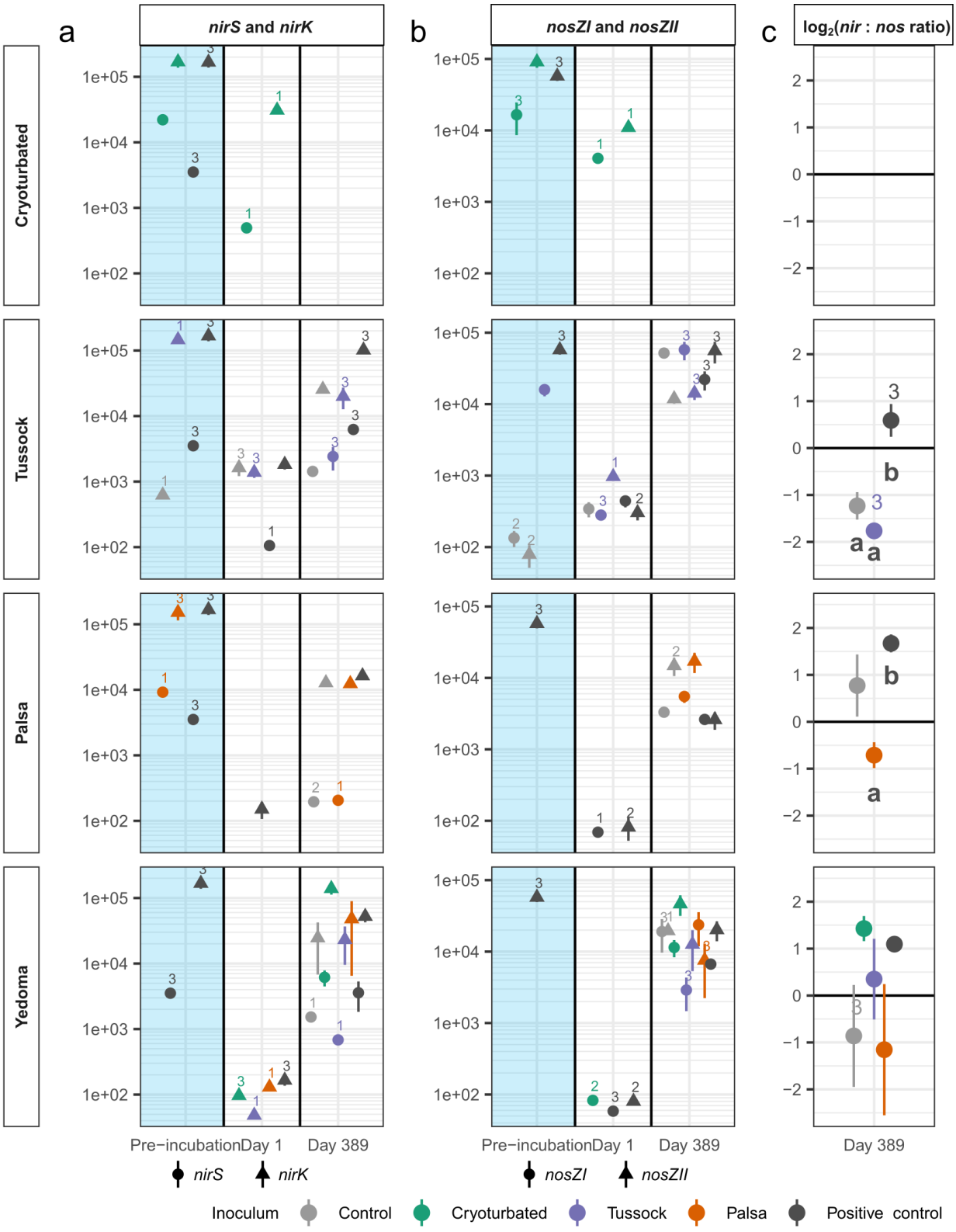

Supplementary Figure S5: Abundance of variants of genes controlling production (nitrite reductase, a) and consumption (nitrous oxide reductase, b) of N_2O as well as their ratio in four permafrost soils subjected to microbial community manipulation after 389 days of oxic incubation.

(**a-b**) gene copy numbers per gram soil dry weight, (**c**) $\log_2$ of the sum of *nirS* and *nirK* divided by sum of *nosZ* clade I and II gene copy numbers expressed per gram soil dry weight. Symbols and error bars depict mean +/- SE (n=4 unless specified otherwise by numbers when below detection limit). In (**c**) horizontal black lines indicate a $\log_2$ ratio of 0, i.e. a ratio of 1 (*nir* = *nos*); ratios computed only where both *nir* and *nos* genes were detected. Different letters denote significant differences within a soil type (EMmeans Holm-adjusted $P < 0.05$).

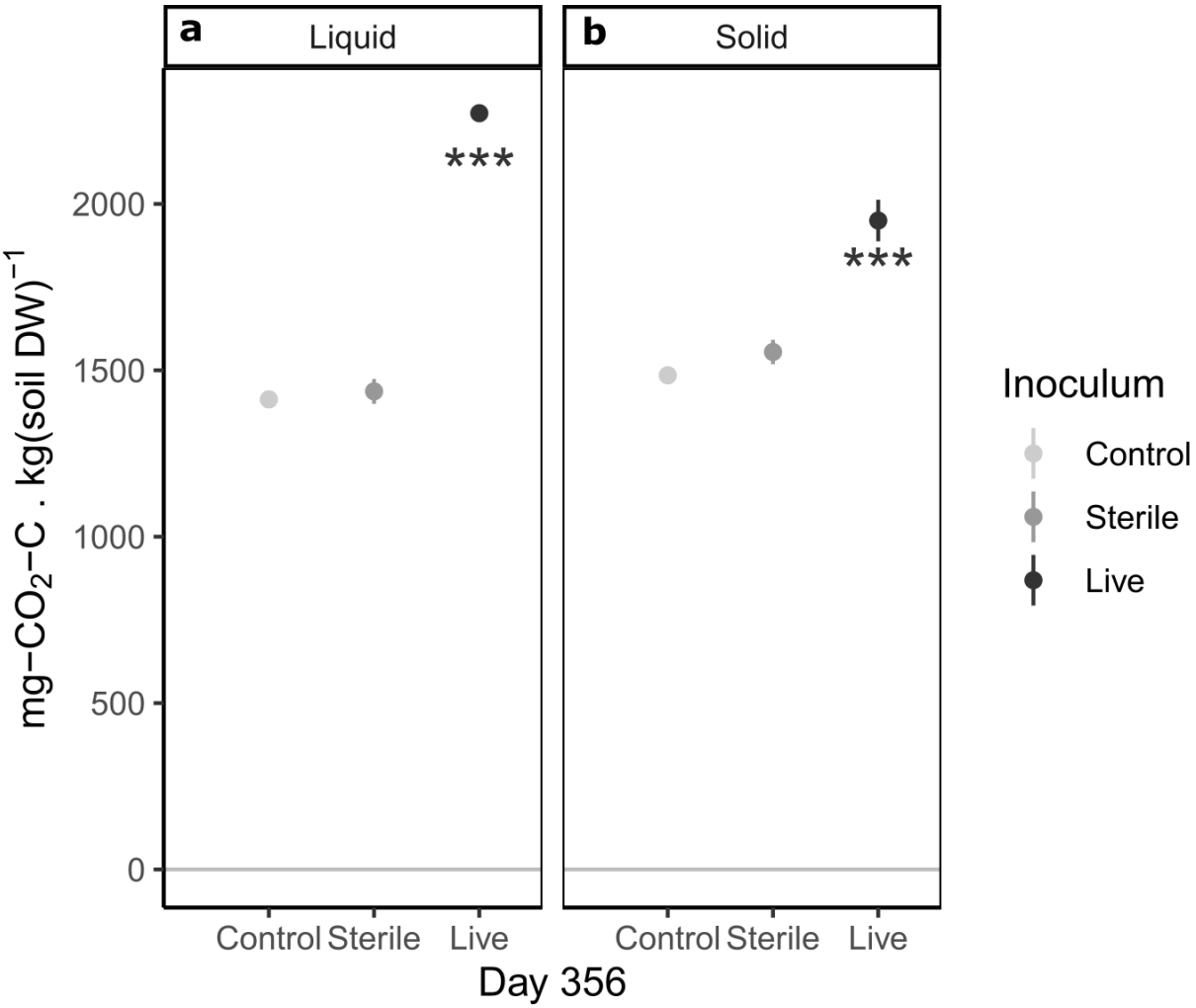

Supplementary Figure S6: Supplementary oxic incubation of Yedoma permafrost to assess artefacts from inoculation.
(a-b): Cumulative CO_2 production of Yedoma permafrost inoculated with the positive control soil (Live) or gamma-irradiated positive control soil (Sterile), after 356 days of oxic incubation. The two panels differ in inoculation method, either with **(a)** 1ml of soil suspension (ddH_2O for Control), or with **(b)** 1.5% weight:weight soil replacement (as in Monteux *et al*., 2020 ref [10]). Symbols and error-bars indicate mean +/- SE (n=4, except Liquid-Sterile where n=3), asterisks denote significant (Holm-adjusted $P < 10^{-4}$) differences from the Control.